Marine Micropaleontology 115 (2015) 24–38

Contents lists available at ScienceDirect

Marine Micropaleontology

journal homepage: www.elsevier.com/locate/marmicro

Research paper

Mediterranean coccolith ecobiostratigraphy since the penultimate Glacial (the last 145,000 years) and ecobioevent traceability

Agata Di Stefano [a], Luca M. Foresi [b], Alessandro Incarbona [c,*], Mario Sprovieri [d], Mattia Vallefuoco [e], Marina Iorio [e], Nicola Pelosi [e], Enrico Di Stefano [c], Patrizia Sangiorgi [a], Francesca Budillon [e]

[a] Università degli Studi di Catania, Dipartimento di Scienze Biologiche, Geologiche e Ambientali, Corso Italia 57, 95129 Catania, Italy
[b] Università degli Studi di Siena, Dipartimento di Scienze Fisiche, della Terra e dell'Ambiente, Strada Laterina 8, 53100 Siena, Italy
[c] Università degli Studi di Palermo, Dipartimento di Scienze della Terra e del Mare, Via Archirafi 22, 90134 Palermo, Italy
[d] Consiglio Nazionale delle Ricerche, Istituto per l'Ambiente Marino Costiero, Via del Mare 3, 91021 Torretta Granitola (Campobello di Mazara, Trapani), Italy
[e] Consiglio Nazionale delle Ricerche, Istituto per l'Ambiente Marino Costiero, Calata Porta di Massa, Interno Porto di Napoli, 80133 Napoli, Italy

ARTICLE INFO

Article history:
Received 19 April 2014
Received in revised form 20 October 2014
Accepted 20 December 2014
Available online 29 December 2014

Keywords:
coccoliths
Mediterranean Sea
late Quaternary
ecobiostratigraphy
ecobioevent traceability

ABSTRACT

The Mediterranean Sea is a miniature ocean ideal to test the response of marine ecosystems to amplified orbital and suborbital climate changes. Here we present coccolith data from a Sardinia Channel gravity core (Arcose C_33) analysed over the last 145,000 years, with a mean resolution of about 900 years. The study highlights that regional phytoplankton assemblages underwent significant modifications between the penultimate glacial and the last interglacial, as well as between the last glacial and the Holocene. The *N* ratio palaeoproductivity index suggests reduced productivity levels and the development of a deep nutricline during the last interglacial and the Holocene. Within the last glacial period, many taxa exhibit abundance fluctuations that parallel oscillations in $\delta^{18}O$ values of *Globigerina bulloides* tests. Heinrich events and stadials seem to be associated with drops in primary productivity levels, as already observed in the Alboran Sea and the Sicily Channel. A total of 19 ecobioevents were identified in the Sardinia Channel sediments, including abundance fluctuations of *Emiliania huxleyi* >4 μm, *Florisphaera profunda* and *Gephyrocapsa oceanica*. The comparison of events across the Mediterranean Sea suggests that traceability applies to the Sicily Channel, Balearic and Tyrrhenian Seas, supporting the adoption of a common ecobiostratigraphic scheme. Less certain is the correlation with the Alboran Sea, although peaks of *Helicosphaera carteri* and *Syracosphaera histrica* during Heinrich events and stadials suggest similar nutrient dynamics in response to suborbital climatic variations in the Sicily Channel, southern Tyrrhenian and Alboran Seas. The traceability of events within eastern Mediterranean cores is strongly limited, possibly due to different physico-chemical properties and nutrient dynamics.

1. Introduction

Marine environmental variations induced by orbital and suborbital climate changes provide a sequence of regional ecobioevents, such as temporary appearance or disappearance, or significant relative abundance variations, of specific taxa. The definition and validation of ecobiostratigraphic schemes need a comprehensive understanding of causes and timing leading to ecobiostratigraphic events, in the framework of a multidisciplinary stratigraphic research program (Rey and Galeotti, 2008).

The Mediterranean Sea is a miniature ocean ideal to test oceanographic processes at a reasonable spatial scale (Bethoux et al., 1999). Abrupt and rapid (suborbital) climatic oscillations over the last 130 kiloyears (kyr) have been identified in Mediterranean marine and terrestrial records and can be correlated to Greenland and North Atlantic events, possibly because of teleconnection phenomena (e.g., Allen et al., 1999; Cacho et al., 1999; Sprovieri et al., 2003, 2006; Martrat et al., 2004; Frigola et al., 2008; Sprovieri et al., 2012; Toucanne et al., 2012). As a consequence, the Mediterranean region is a suitable location to gather information on the response of marine ecosystems to high-frequency climatic forcing and to assess ecobiostratigraphic schemes for calcareous plankton in the late Quaternary.

The comparison of planktonic foraminifera ecobiohorizons in the latest Quaternary (about the last 20 kyr) sediments shows a high degree of similarity, even in different subbasins, such as the Adriatic Sea, Sicily Channel and Tyrrhenian Sea (Lirer et al., 2013). Such an attempt is so far missing for coccolithophores, unicellular marine planktonic algae belonging to the phylum Haptophyta that constitute one of the most important contributors to calcium carbonate in the ocean since the Late Triassic (Bown, 1998). Numerous studies, from different climatic/oceanographic settings, highlight the utility of this group in revealing surface water dynamics at both orbital- and suborbital-scales (e.g.,

* Corresponding author. Tel.: +39 091 23864648.
E-mail address: alessandro.incarbona@unipa.it (A. Incarbona).

http://dx.doi.org/10.1016/j.marmicro.2014.12.002
0377-8398/

Molfino and McIntyre, 1990; Beaufort et al., 1997; Rogalla and Andruleit, 2005; Di Stefano et al., 2010; Incarbona et al., 2010a). However, as summarized in Table 1, late Quaternary coccolith palaeoenvironmental studies in the Mediterranean Sea have been carried out on limited time domains (e.g., Sbaffi et al., 2001; Colmenero-Hidalgo et al., 2004; Di Stefano and Incarbona, 2004) and the longest record was indeed focused on sapropel layers (Negri et al., 1999).

The present paper is aimed at realising the first Mediterranean ecobiostratigraphic zonation, based on coccoliths, over the last 145 kyr (including the MIS 6/MIS 5 transition, the last glacial period, the last glacial/Holocene transition and the Holocene) carried out in the Sentinelle Valley record: i) we identify ecobiohorizons and evaluate their timing, including the associated error estimate; ii) we link events to late Quaternary climatic variations, after providing a high-resolution palaeoenvironmental reconstruction; and iii) we compare bioevents identified in the Sentinelle Valley record to those from different Mediterranean areas, to assess whether coccolith assemblages were modified in response to the same climatic forcing and thus evaluating possible diachroneity.

2. Oceanographic setting

The Mediterranean Sea conveyor belt is formed of three layers. Surface waters, called Modified Atlantic Water (MAW), enter from the Atlantic Ocean (Fig. 1) and undergo strong evaporation and mixing processes while they flow eastward (POEM group, 1992; Malanotte-Rizzoli et al., 2014). MAW describes a quasi-permanent anticyclonic gyre in the western Alboran Sea and flows along the North African coast as the Algerian Current (Millot, 1999; de Jesús Salas Pérez, 2003). At the entrance of the Sicily Strait, surface water separates into the Tyrrhenian Sea and the Sicily Channel. The flows of MAW west and east of Corsica join and form the Liguro–Provençe–Catalan Current (Millot, 1999). A very intense thermal front is developed between the Gulf of Lions, where the cool Northwesterlies blow, and the Balearic Sea that is far less windy (Millot, 1999). Part of the Liguro–Provençe–Catalan Current continues southward from the Channel of Ibiza and tends to enter the Alboran Sea where it encounters the energetic flow of recent MAW (Millot, 1999). Into the Sicily Channel, MAW is again split into two streams, southeast of Pantelleria (Robinson et al., 1999; Béranger et al., 2004): the Atlantic Tunisian Current follows the 200 m isobath, reaching the African coast and flowing eastwards as a coastal current (Béranger et al., 2004). The northern branch, called the Atlantic Ionian Stream (AIS), contributes to the MAW transport into the eastern Mediterranean off the southern coast of Sicily. AIS meanders into the Ionian Sea and feeds the Mid-Mediterranean Jet that flows in the central Levantine Basin up to Cyprus. Here, it turns northward, becoming the Cilician Current and the Asian Minor Current (POEM group, 1992; Pinardi and Masetti, 2000). The strong fragmentation in quasi-permanent anticylonic (such as Syrte, Mersa–Matruh and Shikmona) and cyclonic (such as Rhodes and Cretan) gyres testifies the strong sub-basin scale activity.

Levantine Intermediate Water (LIW) forms in the eastern basin in February–March as a process of surface cooling on water masses which underwent a severe salt enrichment, in a limited area between Rhodes and Cyprus and occupies a depth between 150–200 and 600 m (Ovchinnikov, 1984; Malanotte-Rizzoli and Hecht, 1988). Dense water forms in the northern part of the basin, in the Gulf of Lions, and in the Adriatic and Aegean Seas (POEM group, 1992; Millot, 1999).

Water column dynamics in the Mediterranean Sea control seasonal changes in primary production. The winter convection, and less frequent frontal zones or upwelling areas, bring nutrients into the photic zone (mesotrophic regime) (Klein and Coste, 1984). LIW is the carrier of nutrients in the upper part of the water column for fertilization (Krom et al., 2010). An oligotrophic regime, characterized by a much lower level of production, occurs in summer, when a stable stratification, due to the deepening of the summer thermocline up to about 90 m, takes place (Klein and Coste, 1984; Krom et al., 1992).

A significant West–East trophic gradient exists and is associated with a significant nutrient depletion (mainly phosphorus) and a reduction in primary productivity in the eastern basin (Krom et al., 1991, 2010). Moreover, primary productivity reflects the hydrological fragmentation at both subbasin- and meso-scale variability (D'Ortenzio and Ribera d'Alcalà, 2009).

In the Sardinia Channel the upper part of the water column, corresponding to the photic zone, is occupied by 150–200 m of MAW (Astraldi et al., 1999, 2002). The study area is classified as a 'non blooming' region by D'Ortenzio and Ribera d'Alcalà (2009), that is an oligotrophic region with a distinct seasonal pattern characterised by low biomass during late spring–summer and higher biomass in late fall–winter. However, there are reports of temporary upwelling and small-scale cyclonic gyres that make surface water colder and more productive (Sammari et al., 1999; Onken and Sellschopp, 2001; Astraldi et al., 2002).

3. Material

Arcose C_33 core was obtained from the Sentinelle Valley (38°39.486′N, 10°20.982′E, 2368 m water depth), in the Sardinia Channel, at the edge with the western-southern Tyrrhenian Sea (Fig. 1), during the homonymous CNR cruise onboard the R/V Urania in September 2010. This area was firstly investigated during the CIESM Sub2 cruise realised in December 2005, during which the nearby Core C08 was obtained (Budillon et al., 2009).

The gravity core is 6.57 m long and the sediment is composed of generally homogeneous grey clays, sometimes thinly laminated or banded. Brown or black layers mm- and cm-thick are randomly present through the whole sequence. Sporadic sandy layers are also present, the thicker of which, recorded between 4.01 and 4.09 mbsf, is characterised by well-classed coarse grains. A detailed lithostratigraphic and sedimentological log is shown in Fig. 1 of Supplementary material.

Table 1
List of relevant palaeoenvironmental studies based on coccoliths in the Mediterranean Sea: from the left: bibliographic reference; core's name/code; geographical setting; time domain; average resolution.

Paper	Cores	Area	Time domain (kyr)	Mean resolution (years)
Present study	ARC33	Tyrrhenian	130–0	700
Incarbona et al. (2013)	ODP Site 963	Sicily Channel	70–20	100
Incarbona et al. (2010c)	ODP Site 963	Sicily Channel	135–65	160
Triantaphyllou et al. (2009)	NS-14	Aegean	14–0	90
Incarbona et al. (2008a)	LC07	Sicily Channel	145–20	400
Colmenero-Hidalgo et al. (2004)	MD95-2043	Alboran	50–0	500
Di Stefano and Incarbona (2004)	ODP Site 963	Sicily Channel	20–0	50
Sbaffi et al. (2001)	BS79-33	Tyrrhenian	30–0	700
Negri et al. (1999)	M25/4-12	Ionian	350–0	2800
Flores et al. (1997)	K1 and K10	Balearic	100–0	2000

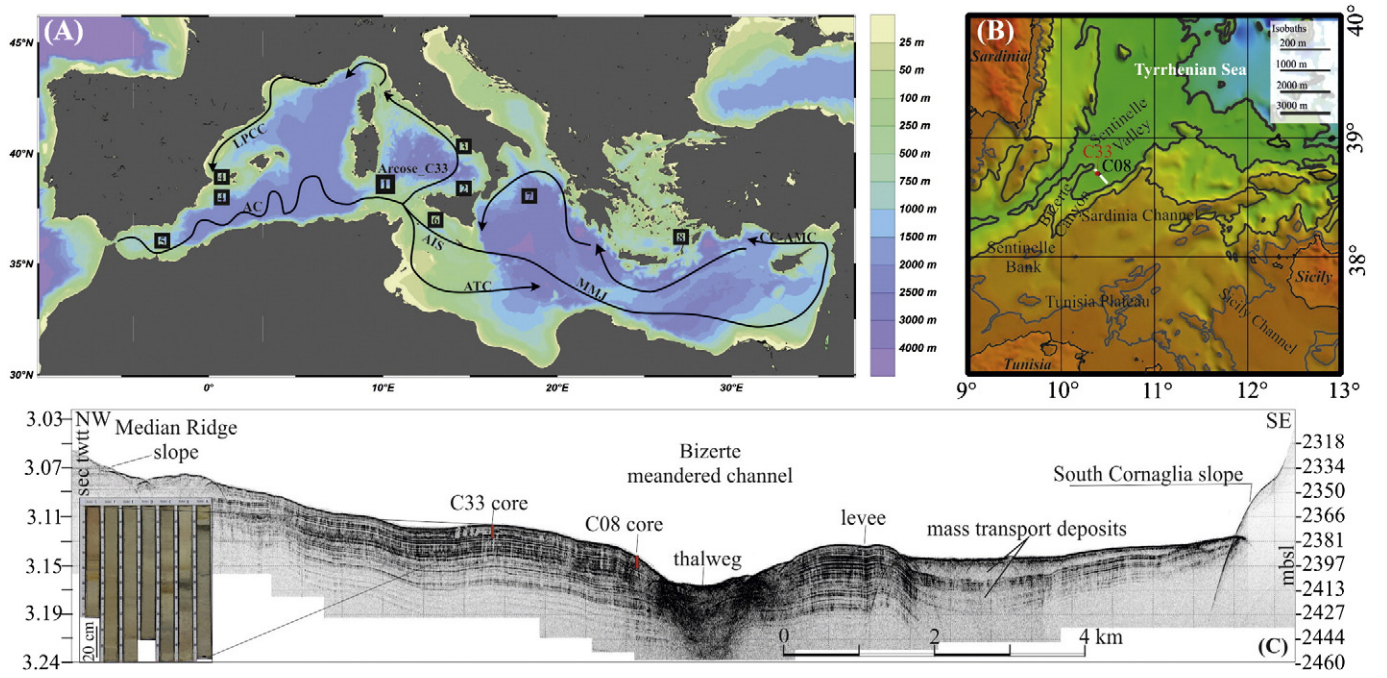

Fig. 1. (A) Bathymetric map of the Mediterranean Sea; black arrows show the path of surface water circulation (modified from POEM group, 1992 and Pinardi and Masetti, 2000). The acronyms of surface currents are also indicated: LPCC, Liguro–Provençe–Catalan Current; AC, Algerian Current; AIS, Atlantic Ionian Stream; ATC, Atlantic Tunisian Current; MMJ, Mid-Mediterranean Jet; CC–AMC, Cilician Current and Asian Minor Current. Black squares represent the location of cores discussed in the text: 1) Sardinia Channel, Arcose_C33 (present study) and LC07 (Incarbona et al., 2008a); 2) Tyrrhenian Sea, BS79-33 (Sbaffi et al., 2001); 3) Tyrrhenian Sea, C106 (Buccheri et al., 2002); 4) Balearic Sea, K1 and K10 (Flores et al., 1997); 5) Alboran Sea, MD95-2043 (Colmenero-Hidalgo et al., 2004); 6) Sicily Channel, ODP Site 963 (Di Stefano and Incarbona, 2004; Incarbona et al., 2010c); 7) Ionian Sea, M25/4-12 (Negri et al., 1999); and 8) Aegean Sea, NS-14 (Triantaphyllou et al., 2009); (B) location of Arcose_C33 and Ciesm C08 cores (modified from Budillon et al., 2009); (C) Subbottom chirp line shot across the Sentinelle Valley, where the stratigraphic succession of Arcose_C33 (see left corner photograph) and C08 was obtained.

4. Methods

4.1. Stable isotopes

Oxygen and carbon isotope analyses were carried out on about ten specimens of the planktonic foraminifera species *Globigerina bulloides*. 246 samples were measured by an automated continuous flow carbonate preparation GasBenchII device (Spötl and Vennemann, 2003) and a ThermoElectron Delta Plus XP mass spectrometer at the IAMC-CNR (Naples) isotope geochemistry laboratory. Acidification of samples was performed at 50 °C. An internal standard (Carrara Marble with $\delta^{18}O = -2.43‰$ versus Vienna Pee Dee Belemnite (VPDB) and $\delta^{13}C = 2.43‰$ versus VPDB) was run every six samples, whereas the NBS19 international standard was measured every 30 samples. Standard deviations of carbon and oxygen isotope measurements were estimated at 0.1 and 0.08‰ respectively, on the basis of ~20 repeated samples. Isotope data are reported in per mil (‰) relative to the VPDB standard.

4.2. Coccolith assemblages

Quantitative analysis was carried out on 181 samples using a polarized microscope at 1250× magnification. About 30 taxonomic units were taken into account, following the taxonomic concepts of Young et al. (2003). The 'small placoliths' taxonomic unit included small specimens of *Reticulofenestra* spp., *Emiliania huxleyi* and possibly of the genus *Gephyrocapsa* with broken bridges.

Over 500 specimens were counted on the smear slides, prepared following standard procedures (Bown and Young, 1998). Additional counts were carried out on 100 specimens of *Calcidiscus leptoporus* and *Coccolithus pelagicus*, in order to evaluate their relative abundance. Following the methodology adopted by Fenner and Di Stefano (2004), the analysis was carried out without discerning morphotypes and subspecies (Parente et al., 2004; Quinn et al., 2004). The ratio between the two species revealed a distinct abundance reversal in subantarctic and subtropical sediments of the Pacific Ocean at the MIS 2/1 boundary (Fenner and Di Stefano, 2004).

In order to refine the palaeoecological interpretation, taxa were grouped into 'placoliths', 'miscellaneous group', 'upper photic zone (UPZ) group' and 'lower photic zone (LPZ) group' following Young (1994), Di Stefano and Incarbona (2004) and Incarbona et al. (2010b, 2011). Placoliths included *E. huxleyi*, small *Gephyrocapsa*, *Gephyrocapsa muellerae*, *Gephyrocapsa oceanica* and small placoliths. This group is formed by r-strategist taxa and can be considered as a proxy of high productivity conditions (Young, 1994; Broerse et al., 2000; Flores et al., 2000; De Bernardi et al., 2005; López-Otálvaro et al., 2008). The miscellaneous group consisted of taxa that live without any specific depth and/or within a wide range of ecological preferences, specifically *Helicosphaera* spp., *C. pelagicus*, *Syracosphaera histrica*, *Pontosphaera* spp., *C. leptoporus*, *Pleurochrysis* spp., *Braarudosphaera* spp., *Oolithotus fragilis* and specimens of all the other species. The UPZ group included *Syracosphaera pulchra*, *Umbellosphaera* spp., *Discosphaera tubifera*, *Rhabdosphaera* spp., *Umbilicosphaera* spp., *Calciosolenia* spp., holococcoliths, *Ceratolithus* spp. and the dinoflagellate *Thoracosphaera heimii* (Tangen et al., 1982). UPZ taxa are K-strategists, specialized to live in warm subtropical surface waters and to exploit a minimum amount of nutrients (Okada and McIntyre, 1979; Roth and Coulbourne, 1982; Takahashi and Okada, 2000; Andruleit et al., 2003; Boeckel and Baumann, 2004; Baumann et al., 2005). Finally, *Florisphaera profunda* was the most important species belonging to the 'lower photic zone (LPZ) group', that also included *Gladiolithus flabellatus* and *Algirosphaera robusta*, and provides clues on the nutricline depth and on primary productivity levels (Molfino and McIntyre, 1990; Beaufort et al., 1997; Flores et al., 2000; Incarbona et al., 2008b; Grelaud et al., 2012).

The *N* ratio palaeoproductivity index follows Flores et al. (2000) and is based on the relative abundance of surface eutrophic taxa (small Noelaerhabdaceae: *E. huxleyi*, small *Gephyrocapsa*, *G. muellerae* and

small placoliths) versus the relative abundance of the most important species of the LPZ group (*F. profunda*): small Noelaerhabdaceae/(small Noelaerhabdaceae + *F. profunda*). Values close to 1 indicate higher productivity and a shallower nutricline, values close to 0 suggest lower productivity and a deeper nutricline.

The CEX′ dissolution index was performed following Boeckel and Baumann (2004): Number of specimens of (*E. huxleyi* + small *Gephyrocapsa*) / Number of specimens of (*E. huxleyi* + small *Gephyrocapsa* + *C. leptoporus*). Values close to 1 suggest little or no dissolution effects on coccolith assemblages.

4.3. Petrophysical properties and $CaCO_3$ content

Measurements of core physical properties every 1 cm were performed at the IAMC CNR laboratory. Volume magnetic susceptibility (vms) and diffuse reflectance spectra (DRS in %), over the visible spectrum (from 400 to 700 nm) were measured using a Multi Sensor Core Logger (MSCL) equipment (Geotek Ltd.), mounted with an MS2E Barrington point system and a Minolta Spectrophotometer CM 2002. Both analyses, log plotted, were compared to those obtained from core C08 (Budillon et al., 2009), in order to detect similar trends by peak-to-peak correlation, according to their physical properties and corresponding stratigraphy (Iorio et al., 2014).

The calcium carbonate content was evaluated on 182 samples, using a De Astis Calcimeter (gas-volumetric method), and results were expressed in percentage values.

5. Age model

The age model has been assessed through the tuning of *G. bulloides* $\delta^{18}O$ data on (Fig. 2): i) Greenland ice core data (NGRIP members, 2004), by a peak-to-peak correlation with the Holocene base, the Younger Dryas base and Heinrich events H1–H6, down to about 60 kyr and ii) LR04 benthic stack curve (Lisiecki and Raymo, 2005), importing the age of marine isotopic stage boundaries (MIS 6/5 and 5/4) and substages (within MIS 5). An interpolating cubic spline function was applied, to ensure limited loss of amplitudes at higher frequencies and reduced bias effect (Schulz and Statteger, 1997). The chronology of the uppermost part of the core is constrained by correlation of petrophysical parameters (magnetic susceptibility and colour reflectance), measured every 1 cm, with the nearby CIESM C08 core (Fig. 2 of Supplementary material). The 44 cmbsf level of CIESM C08 core, with a ^{14}C-AMS calibrated age of 8.8 kyr (Budillon et al., 2009), can be correlated to 32 cmbsf in the Arcose C_33 core. Adopted tie-points are listed in Table 2.

The age model was assessed in a composite manner, importing ages from both Greenland ice cores and the LR04 benthic stack curve, in order to get error estimates for the lower stratigraphic interval. In fact, no estimates of age errors exist in Greenland ice core layers older than 57.3 kyr (NGRIP members, 2004). An alternative age model was built by the peak-to-peak correlation with Greenland ice core data, thus including MIS 5 Stadials S25–S20 among tie-points. The resulting chronology does not significantly differ from that used in Fig. 2, as shown by the high parallelism of the two depths versus age plots and

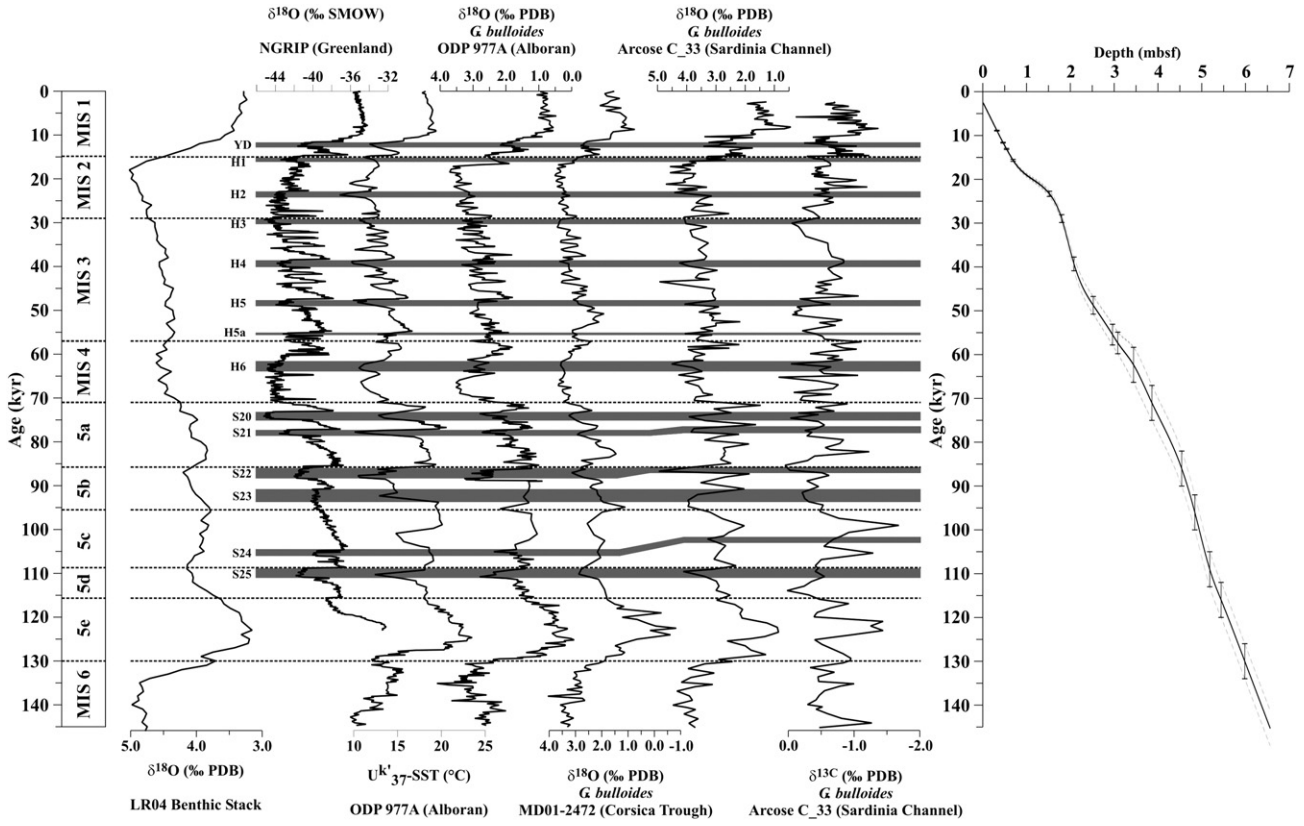

Fig. 2. Geochemical data in the Arcose_C33 core and depth versus age plot. From the left, the core sections and downcore variations versus age of: $\delta^{18}O$ LR04 benthic stack curve (Lisiecki and Raymo, 2005), used as a target for the age model assessment of tie-points older than about 60 kyr; $\delta^{18}O$ of Greenland ice cores (NGRIP members, 2004), used as a target for the age model assessment of tie-points younger than about 60 kyr; SST alkenone-derived in the ODP 977A Hole (Martrat et al., 2004); *Globigerina bulloides* $\delta^{18}O$ values in the Alboran Sea and Corsica Trough (Martrat et al., 2004; Toucanne et al., 2012). *Globigerina bulloides* $\delta^{18}O$ and $\delta^{13}C$ values in the Sardinia Channel (present work); on the right, the depth (mbsf) versus age (kyr) plot. The error estimate (dashed grey line) is shown for each adopted tie-point (Table 2). Columns on the left and dashed black lines show the division into marine isotopic stages and substages. Dark grey bands correspond to Heinrich events and MIS 5 cold spells. YD: Younger Dryas; H1–H6: Heinrich events; S25–S20: MIS 5 cold spells.

Table 2
General information on the age model assessment. From the left: adopted tie-points; depth of each tie-point (cmbsf); age (kyr) of each tie-point, imported from Lisiecki and Raymo (2005) for marine isotopic stage and substage boundaries and from Greenland ice cores (NGRIP members, 2004) for the Holocene base and Heinrich events; estimates of the error for each tie-point derived from the original age model; sedimentation rate (cm/kyr) between tie-points; resolution (years) between tie-points referred to the calcareous nannofossil analysis carried out (generally) every 4 cm.

	Depth (cmbsf)	Age (kyr)	ERROR (± kyr)	Sedrate (cm/kyr)	Resolution (yr × 1 cm)
AMS 14C	32.0	8.80	0.0970		
				5.09	196.4
Hol base	46.0	11.55	0.0970		
				5.52	181.3
YD base	54.0	13.00	0.1400		
				5.77	173.3
S2a (H1)	69.0	15.60	0.2240		
				10.85	92.2
S3 (H2)	152.0	23.25	0.5915		
				4.96	201.8
S5 (H3)	180.0	28.90	0.8980		
				2.71	369.6
S9 (H4)	208.0	39.25	1.5650		
				4.66	214.8
S13 (H5)	252.0	48.70	2.0070		
				6.57	152.3
S15 (H5a)	296.0	55.40	2.3680		
				6.32	158.3
MIS 4/3	308.0	57.30	2.4690		
				7.20	138.9
S18 (H6)	344.0	62.30	4.0000		
				4.83	207.1
MIS 5/4	386.0	71.00	4.0000		
				4.53	220.6
MIS 5b/5a	454.0	86.00	4.0000		
				3.00	333.3
MIS 5c/5b	484.0	96.00	4.0000		
				2.62	382.4
MIS 5d/5c	518.0	109.00	4.0000		
				3.71	269.2
MIS 5e/5d	544.0	116.00	4.0000		
				3.86	259.3
MIS 6/5	598.0	130.00	4.0000		

the very similar polynomial regression lines (Fig. 3 of Supplementary material).

Following the age model, sedimentation rates range between 2.6 and 10.8 cm/kyr (Table 2), with a mean value of 4.6 cm/kyr. These values are comparable with other late Quaternary records of the Sardinia Channel (Incarbona et al., 2008a; Budillon et al., 2009). The sampling resolution for coccolith analysis is 870 years on average, between 369 and 1530 years up to 0.72 mbsf and less than 400 years in the uppermost part of the record where samples were collected every 2 cm. The estimated age of the top sample is 2.35 kyr and suggests the loss of the most recent sedimentary material as documented in the CIESM C08 core (Budillon et al., 2009).

6. Results

6.1. Stable isotopes

Oxygen isotope data, acquired on the tests of *G. bulloides*, range between 0.5 and 5.0‰. These values are slightly heavier than those reported for the same species from late Quaternary records of the western Mediterranean Sea, where they are between 0.0 and 4.5‰ (Cacho et al., 1999; Martrat et al., 2004; Sierro et al., 2005; Toucanne et al., 2012), possibly due to the evaporation and salt enrichment of MAW during its westward path (Fig. 1) and/or to small-scale upwelling-type phenomena in the Sardinia Channel (Sammari et al., 1999; Onken and Sellschopp, 2001; Astraldi et al., 2002). However, the $\delta^{18}O$ profile and high-frequency oscillations presented in Fig. 2 are comparable to sea surface temperature (SST) and $\delta^{18}O$ curves from the Alboran Sea and Corsica Trough, despite minor misalignments in MIS 5 stadials (Fig. 2).

Dark grey bands mark the heaviest oxygen isotopic values (5.0–3.5‰) that identify Younger Dryas, Heinrich events (H1–H6) and MIS 5 cold spells (S25–20) (Fig. 2). The last glacial period is characterised by high-frequency oscillations between 0.5 and 2.0‰ which are suggestive of Dansgaard–Oeschger oscillations and light grey bands indicate some of the stadials (Fig. 3). The relatively low-resolution of the Arcose C_33 core (about 900 years on average) prevents the identification and numbering of the whole sequence of events. However, in the uppermost part of the record, during Termination I where the $\delta^{18}O$ analysis was carried out every 1 cm (resolution of about 180 years), there is little doubt that the Bolling–Allerød and Younger Dryas can be readily recognized (Fig. 2).

$\delta^{13}C$ values range between −2.0 and 0.0‰, showing high and rapid variability. Generally, the lowest values of $\delta^{13}C$ are associated with light values in $\delta^{18}O$ and vice versa (Fig. 2). Especially during the last glacial, short-term fluctuations suggest rapid changes in seawater conditions.

Stable isotope raw data are available in Table 1 of Supplementary material.

6.2. Coccolith assemblages

Coccoliths are always abundant and well-preserved. Assemblages are dominated by gephyrocapsids (*G. muellerae* and small *Gephyrocapsa*) up to 46.1 ± 1.9 kyr BP (Plate I, A–B) and by *E. huxleyi* in the remaining part of the record (Plate I, C) (Fig. 3). Gephyrocapsa *muellerae* relative abundance ranges between 0 and 85%, with higher abundances in the lowermost part of the record up to about 125.2 ± 4.0 kyr BP and from MIS 5d to the lower part of MIS 3 (Fig. 3). Small *Gephyrocapsa* percentage values range between 0 and 50%. There is some significant anticorrelation with *G. muellerae* during MIS 6 and the lower part of MIS 5 and few significant peaks occur up to MIS 4 (Fig. 3). *E. huxleyi* <4 μm shows a gradual increase since 62.3 ± 4.0 kyr BP. After a marked decrease during MIS 2, this morphotype occurs with values between 55 and 80% during Termination I and the Holocene (Fig. 3). *E. huxleyi* >4 μm occurs with wide abundance fluctuations (~20% of maximum value) between 63.0 ± 4.1 and 15.1 ± 0.2 kyr BP (Plate I, D–E) (Fig. 3). *F. profunda* is abundant, up to 45%, during the two interglacial intervals, but peaks of a much lower magnitude can be observed throughout the remaining part of the record (Plate I, F–G) (Fig. 4). All the other taxa occur with percentage values lower than 10% and exhibit distinctive peaks (Figs. 3–5), such as *C. leptoporus*, *S. pulchra*, *Pleurochrysis* spp. (Plate I, H–J) and *Umbellosphaera* ssp., or a distinctive interglacial occurrence, such as *G. oceanica* and *Umbilicosphaera sibogae* (Plate I, C). The only exception is represented by holococcoliths, whose abundance, mostly due to specimens of *S. pulchra* HOL *oblonga* (*Calyptrosphaera oblonga*) (Plate I, I–L), ranges between 0 and 25% (Fig. 4). To our knowledge, it is the first time that *Pleurochrysis* spp. and *S. pulchra* HOL *oblonga* were significantly recorded in sedimentary cores and were used for ecobiostratigraphic purposes.

About the additional counting on *C. leptoporus* and *C. pelagicus*, the former species is always dominant, apart from a short interval within MIS 5. However, several peaks of *C. pelagicus* are present throughout the core, especially during MIS 3 and Termination I (Fig. 6).

Raw data and percentage values of coccolith taxa, together with the additional counting, are available in Table 1 of Supplementary material.

6.3. Petrophysical properties and $CaCO_3$ content

The petrophysical result was already illustrated in Section 5.1 and deals with the correlation of the uppermost CIESM C08 and Arcose C_33 sediments, and the age assignment of 8.8 kyr to the 32 cmbsf depth in the latter core. In general, the offset between correlation lines of the two Sentinelle Valley cores is throughout limited to a few tens of centimetres (Fig. 2 of Supplementary material), likely due to their

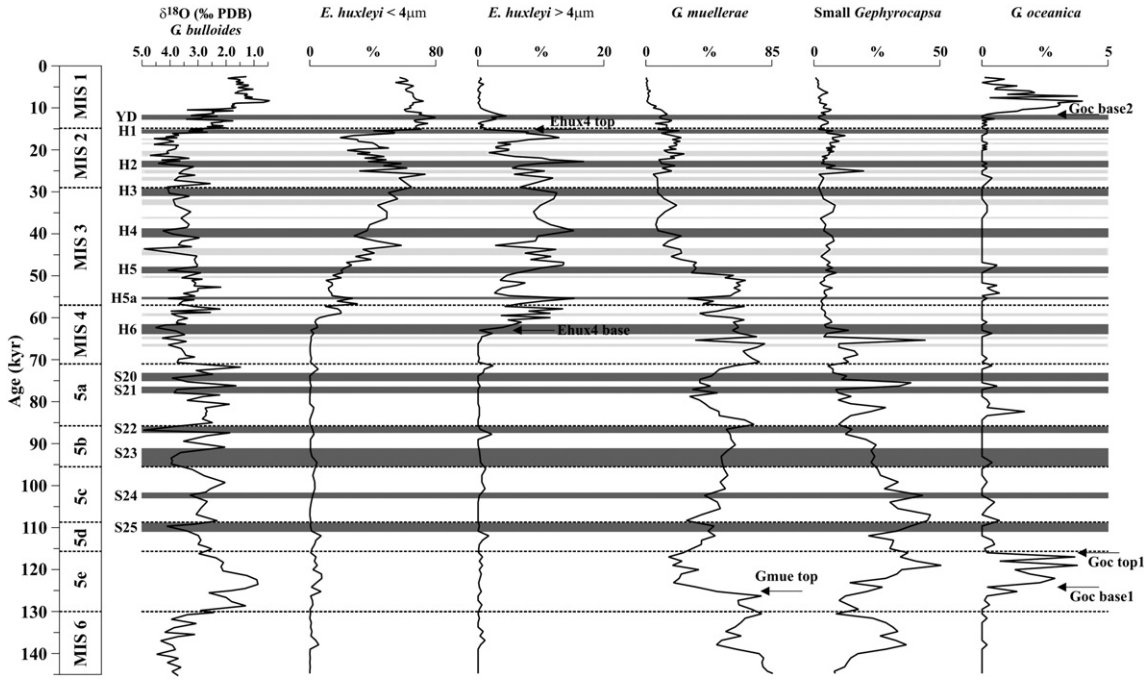

Fig. 3. Geochemical and micropaleontological data in the Arcose_C33 core. From the left, downcore variations versus age of *G. bulloides* $\delta^{18}O$ values and selected coccolith taxa belonging to placoliths. Columns on the left and dashed black lines show the division into marine isotopic stages and substages. Dark grey bands correspond to Heinrich events and MIS 5 cold spells, light grey bands to stadials. YD: Younger Dryas; H1–H6: Heinrich events; S25–S20: MIS 5 cold spells; Ehux4 base: *E. huxleyi* >4 μm base; Ehux4 top: *E. huxleyi* >4 μm top; Gmue top: *G. muellerae* top; Goc base1: *G. oceanica* base in the last interglacial; Goc top1: *G. oceanica* top in the last interglacial; Goc base2: *G. oceanica* base in the Holocene.

close proximity. A pretty good match is observed between −0.05/−1.60 m (corresponding to −0.15/−1.80 m in core C08) and −2.34/−4.64 m (corresponding to −284/−5.25 m in core C08). The offset increases toward the core bottom for the occurrence of several cm- to dm-thick sandy turbidites in core C08, as the result of the activity of the nearby Bizerte Canyon (Fig. 1). On the whole, core C33 entered the sedimentary succession approximately 1.35 m deeper (−5.25/−6.60 m) than core C08, thus recording a much longer stratigraphic interval.

The calcium carbonate content in the sediment is quite variable, between 66.9 and 22.4% and several peaks can be noted throughout the record (Fig. 6).

Calcium carbonate raw data are available in Table 1 of Supplementary material.

7. Discussion

7.1. Palaeoproductivity reconstruction

In order to reveal the palaeoecological meaning of coccolith assemblages, taxa are considered as grouped and described in Section 4.2.

7.1.1. Interglacials and terminations

At the Sentinelle Valley Site, Termination II is characterised by a lightening in oxygen isotopic values at the MIS 6/MIS 5 boundary, followed by a marked shift toward heavier values (Fig. 7) as already noted in the most oceans (e.g., Oppo, 1997; Shackleton et al., 2003). The turnover in the floral assemblages, happened just after this second event with the sharp increase of LPZ taxa (*F. profunda*) at the expense of the placoliths, points to reduced productivity levels and the development of a deep nutricline (Molfino and McIntyre, 1990; Young, 1994; Beaufort et al., 1997; Broerse et al., 2000; Flores et al., 2000; Incarbona et al., 2008b). Moreover, among placoliths, small *Gephyrocapsa* replaced *G. muellerae* supporting the occurrence of warmer and/or nutrient-depleted surface waters (Pujos, 1988; Flores et al., 1997; Henriksson, 2000; Baumann and Freitag, 2004; Incarbona et al., 2010c). Initial conditions, like those of MIS 6 and of Termination II, with high abundances of placoliths (*G. muellerae*) and low abundances of *F. profunda*, are restored in coincidence of the Stadial S25, co-occurring with a 1.5‰ enrichment in $\delta^{18}O$ values (Fig. 7). This horizon marks the end of the last interglacial sensu lato (Sanchez Goñi et al., 1999; Shackleton et al., 2003) that includes part of MIS 5e and part of MIS 5d.

Termination I is characterised by the sequence of a warm (Bolling–Allerød) and a cold (Younger Dryas) suborbital fluctuation that are readily identified in our record by both $\delta^{18}O$ and coccolith data (Fig. 7). Likewise the last interglacial sensu lato, at the base of the Holocene there is an increase of LPZ (*F. profunda*) and a decrease of placoliths (Fig. 7), that again suggest reduced productivity and the development of a deep nutricline (Molfino and McIntyre, 1990; Young, 1994; Beaufort et al., 1997; Broerse et al., 2000; Flores et al., 2000; Incarbona et al., 2008b), gradually strengthened toward the top of the record.

The abundance increase of *F. profunda* during MIS 5e and MIS 1 suggests the development of a distinct deep chlorophyll maximum (DCM). This process resembles the nutricline uplift into the photic zone observed in the eastern Mediterranean sapropels S5 and S1 (Castradori, 1993b; Incarbona et al., 2011; Grelaud et al., 2012). However, living coccolithophore in water samples collected in the central and western Mediterranean Sea show that the *F. profunda* DCM is established because of a different mechanism, the deepening of the summer thermocline down to the lower photic zone (Knappertsbusch, 1993; Bonomo et al., 2012). A weakened coccolith DCM may also be ascribed to the MIS 5b–5a interval (Fig. 7), as already noted in the palaeoenvironmental reconstruction of the nearby LC07 core (Incarbona et al., 2008a).

7.1.2. Glacials and the response to suborbital climatic fluctuations

Higher productivity conditions can be hypothesized during MIS 6 and the last glacial period, at least taking into account the average percentage values of placoliths (Fig. 7). However, within the last glacial period, and especially during MIS 3 and MIS 2, repeated abundance fluctuations in all coccolith groups punctuate the record. In comparison

with $\delta^{18}O$ values of *G. bulloides*, the abundance of placoliths seems to be drastically reduced during stadials, while LPZ, UPZ and Miscellaneous groups increased (Fig. 7).

Helicosphaera carteri, *S. histrica* and *Pleurochrysis* spp., the Miscellaneous taxa, quite regularly increase during MIS 3 and MIS 2 cold spells (Fig. 5) and replace significant amount of placoliths (mostly *E. huxleyi*, Fig. 3). Their ecological preference is not still well-established. For instance, pulses of *H. carteri* and *S. histrica* have been associated with low salinity and surface water turbidity (Giraudeau, 1992; Colmenero-Hidalgo et al., 2004; Grelaud et al., 2012). In any case, they would indicate lower productivity conditions, rather than being proxies of winter/spring bloom like *E. huxleyi* and gephyrocapsids (e.g., Young, 1994; Flores et al., 2000; De Bernardi et al., 2005). Despite only minor fluctuations in the *N* ratio (Fig. 7), and thus the maintenance of a shallow nutricline, surface coccolith productivity seems to be significantly reduced during the last glacial cold phases. This interpretation supports previous studies carried out in the Alboran Sea and in the Sicily Channel and highlights the same response of marine ecosystems to high-frequency climatic fluctuations in a wide sector of the central-western Mediterranean Sea (Cacho et al., 2000, 2002; Pérez-Folgado et al., 2003; Colmenero-Hidalgo et al., 2004; Moreno et al., 2004, 2005; Incarbona et al., 2013). Specifically, the strong vertical gradient density in the upper part of the water column and the inflow of fresher water of polar origin during stadials and Heinrich events, may have disturbed vertical convection and the surface water nutrient replenishment (Incarbona et al., 2013).

A further strong evidence of decreased productivity during MIS 3 and MIS 2 cold spells is the correlation between Miscellaneous taxa and holococcoliths (*S. pulchra* HOL *oblonga*) (Figs 4 and 5), that are typical of warm and oligotrophic water and in fact they are especially abundant in the eastern Mediterranean Sea (e.g., Kleijne, 1991; Knappertsbusch, 1993; Winter et al., 1994; Crudeli et al., 2006; Malinverno et al., 2009). The high preservation potentiality of this species has already been reported in late Quaternary Mediterranean sediments, where it occurs with percentage values up to 25–30% (Crudeli et al., 2006). However, we note that Crudeli et al. (2006) ruled out from their quantitative counts specimens of *E. huxleyi*, gephyrocapsids and *F. profunda*. Thus the abundance reported in the present study for *S. pulchra* HOL *oblonga* may even be higher than in the eastern Mediterranean cores. The palaeoecological signal of holococcoliths in the sedimentary record of the Sentinelle Valley is questioned on the basis of the disproportional abundance and needs an in-depth examination. Holococcoliths are very prone to dissolution because of the crystallographic arrangement (e.g., Roth and Coulbourne, 1982) and their reduced abundance during recent anoxic layers in the eastern Mediterranean has been ascribed to dissolution (Crudeli et al., 2006; Principato et al., 2006). Selective preservation in the Arcose C_33 core may have acted over Stadial/Interstadial cycles and would have decreased the abundance of holococcoliths during interstadials. The western Mediterranean Basin experienced periods of decreased intensity of the thermohaline circulation, associated with a low deep water ventilation and a better preservation of the organic matter during interstadials (Cacho et al., 2000), but no indication exists about the corrosiveness of this water to calcium carbonate.

In order to test the preservation degree of coccolith assemblages in the Sardinia Channel, we superimposed the CEX′ dissolution curve with the distribution curve of holococcoliths (Fig. 4). The CEX′ dissolution index shows very high values (close to 1) throughout the core and especially for the last 60 kyr BP, where holococcoliths occur, the average value is 0.988 (Table 1 of Supplementary material), suggesting very low dissolution processes and supporting the genuine palaeoecological nature of the signal. Alternatively, the CEX′ dissolution index may be not sensitive enough to solve the improved seafloor calcium carbonate preservation during the MIS 3-2 interval.

Finally, $CaCO_3$ variations have often been linked to climatic variations related in turn to productivity changes (e.g., Hilgen, 1987, 1991), but we do not observe a regular pattern in our record (Fig. 6), such as between glacial and interglacial conditions and between suborbital variations. We suspect that the $CaCO_3$ pattern is strongly influenced by aeolian and river terrigenous inputs that may have diluted $CaCO_3$ deposition. This explanation is in fact suitable for the $CaCO_3$ increase that can be observed during the Holocene, where the combined effect of sea-level rise and arboreal vegetation cover may significantly have hindered erosion and transport of terrigenous material.

7.2. Traceability of ecobiostratigraphic horizons

A total of 19 ecobiohorizons can be recognized in the last 145 kyr BP of the Sardinia Channel sedimentary record, and they are listed in Table 3. Events are identified on the basis of statistically significant abundance fluctuations, that is they exceed the error associated with 500 coccolith counts for a 95% confidence level (Table 1 of Supplementary material). In the following, we assess the chronology of each event, estimating the associated error, and test the traceability across the Mediterranean Sea.

7.2.1. Emiliania huxleyi and gephyrocapsids

The *E. huxleyi*/*Gephyrocapsa* reversal (Ehux/Geph rev) is used as a biostratigraphic event in the Mediterranean Sea, to mark the MNN 21a/MNN 21b boundary (Rio et al., 1990). In contrast to ecobiostratigraphic horizons, this event may be affected by the rapid evolutionary development of the *Gephyrocapsa*/*E. huxleyi* phylogenetic lineage (Samtleben, 1980; Rio, 1982; Raffi et al., 1993). We place the event at 46.1 ± 1.9 kyr BP, despite this level is preceded by a short reversal at the MIS 4 base (Fig. 6), like in the Balearic Sea and in the Sicily Channel (Flores et al., 1997; Incarbona et al., 2009, 2013).

The *E. huxleyi*/*Gephyrocapsa* reversal is diachronous in the oceans (Thierstein et al., 1977; Jordan et al., 1996; Villanueva et al., 2002) and different age estimates have also been provided in the Mediterranean Sea (e.g., Castradori, 1993a; Di Stefano, 1998; de Kaenel et al., 1999). However, discrepancies may be due to different methodologies and different approaches for the age model assessment. In any case, the age estimate of the exchange at the Sentinelle Valley site is very close and comparable to the reports from the Balearic Sea, core LC07 and the Sicily Channel (Flores et al., 1997; Incarbona et al., 2008a, 2013).

E. huxleyi >4 μm ecobiohorizons (Ehux4 base and Ehux4 top) define an interval between 63.0 ± 4.1 and 15.1 ± 0.2 kyr BP where this morphotype is evidently abundant, although a smaller peak occurs in coincidence with the Younger Dryas (Fig. 3). Recently, the abundance of *E. huxleyi* >4 μm has been mapped across the North Atlantic and the western Mediterranean (Flores et al., 2010). Percentage values up to 25% are reported in the temperate and subtropical North Atlantic since the Last Glacial Maximum. In the Mediterranean Sea, abundance fluctuations of *E. huxleyi* >4 μm seem to be tightly correlated to Heinrich events in the Alboran Sea, where a significant drop in abundance at the

Plate I. Cross-polarized light images of selected coccolith taxa collected in the Arcose C_33 samples. (A) and (B) assemblages dominated by *G. muellerae* specimens (sample 3, 6.52 mbsf). (C) Specimens of *E. huxleyi* <4 μm (red arrows). Also present in the picture small *Gephyrocapsa*, *G. oceanica* and *U. sibogae* specimens (sample 335, 0.3 mbsf). (D) and (E) specimens of *E. huxleyi* >4 μm (sample 255, 1.48 mbsf). (F) and (G) assemblages dominated by *F. profunda* platelets (red arrows) (sample 43, 5.72 mbsf). (H) specimens of *Pleurochrysis* spp. (sample 271, 1.16 mbsf). (I) specimens of *Pleurochrysis* spp. (white arrow), *S. pulchra* HOL *oblonga* (red arrow) and *H. carteri* (sample 271, 1.16 mbsf). (J) Assemblage including specimens of *Pleurochrysis* spp. (white arrows) and *S. pulchra* HOL *oblonga* (red arrow) (sample 271, 1.16 mbsf). (K) and (L) specimens of *S. pulchra* HOL *oblonga* (sample 271, 1.16 mbsf).

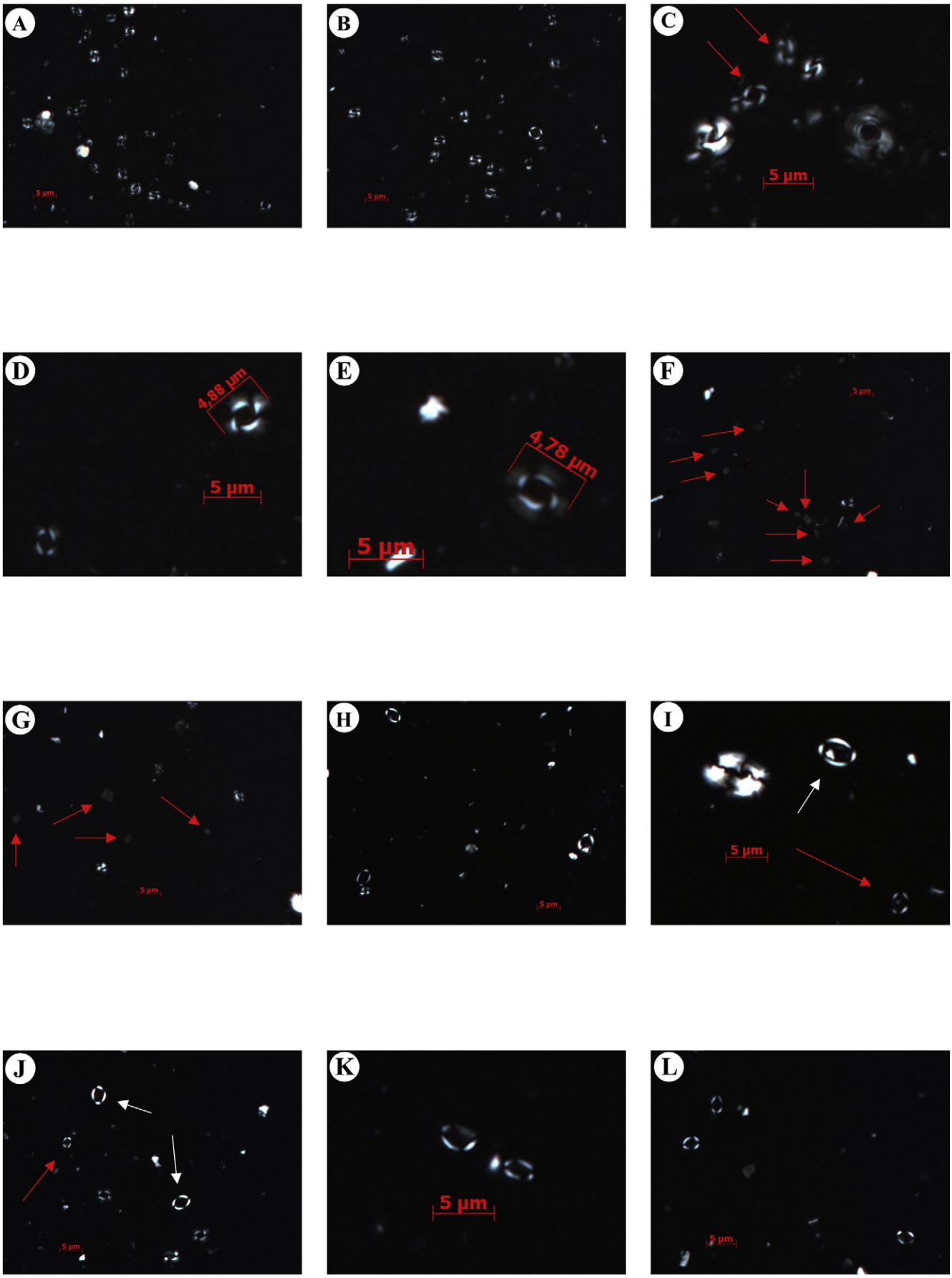
A
5 µm
B
5 µm
C
5 µm
D
4,88 µm
5 µm
E
4,78 µm
5 µm
F
5 µm
G
5 µm
H
5 µm
I
5 µm
J
5 µm
K
5 µm
L
5 µm

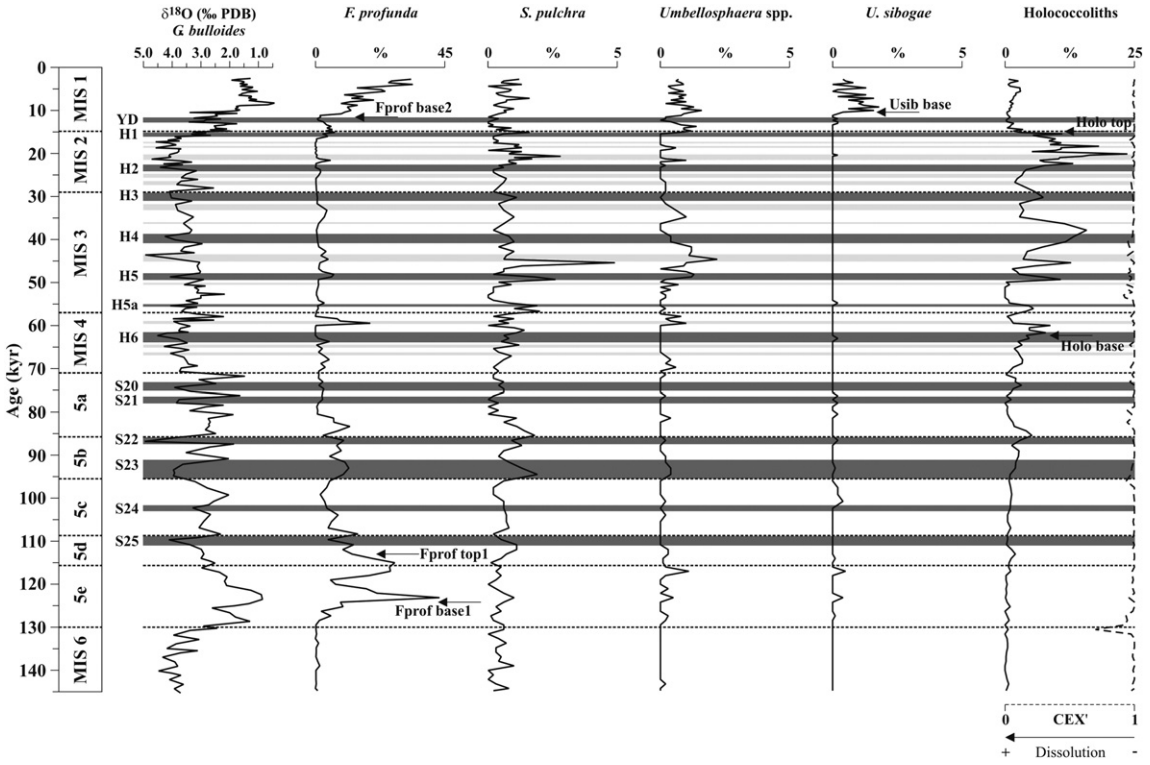

Fig. 4. Geochemical and micropaleontological data in the Arcose_C33 core. From the left, downcore variations versus age of *G. bulloides* $\delta^{18}O$ values and of selected coccolith taxa belonging to the UPZ and LPZ groups. Columns on the left and dashed black lines show the division into marine isotopic stages and substages. Dark grey bands correspond to Heinrich events and MIS 5 cold spells, light grey bands to stadials. YD: Younger Dryas; H1–H6: Heinrich events; S25–S20: MIS 5 cold spells; Fprof base1: *F. profunda* base in the last interglacial; Fprof top1: *F. profunda* top in the last interglacial; Fprof base2: *F. profunda* base in the Holocene; Usib base: *U. sibogae* base; Holo base: holococcoliths base; Holo top: holococcoliths top.

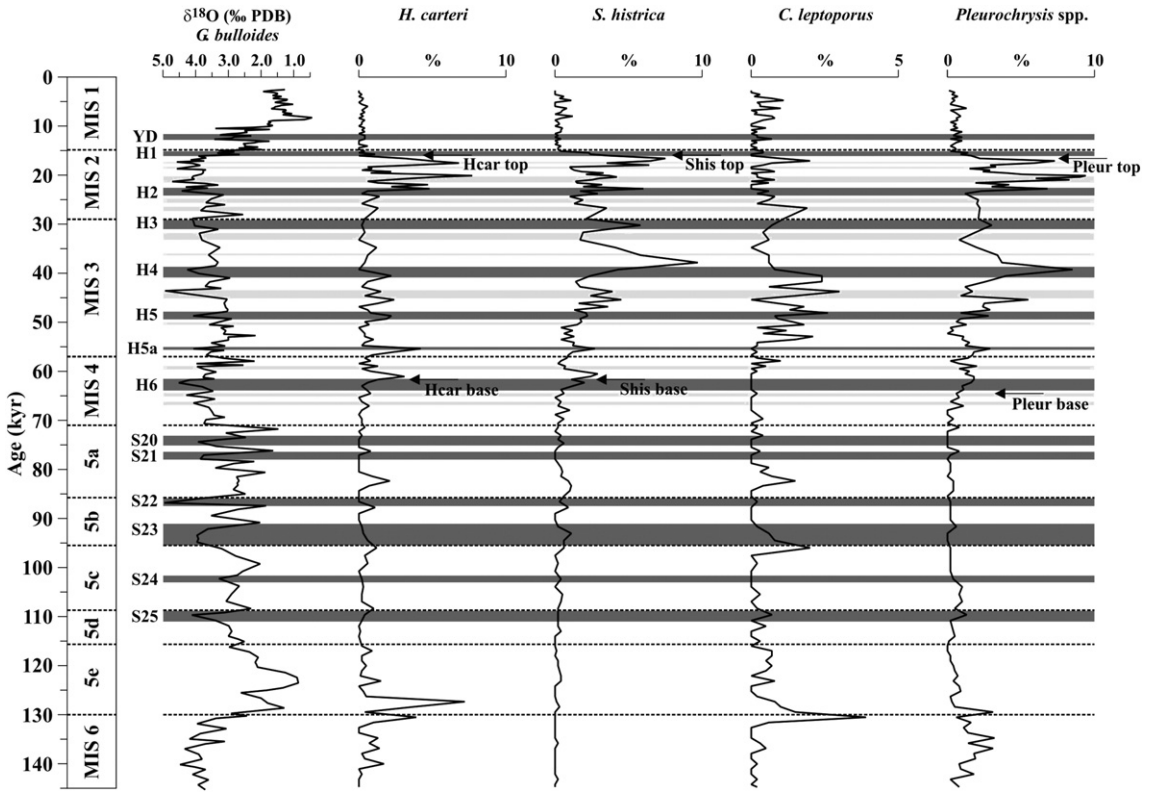

Fig. 5. Geochemical and micropaleontological data in the Arcose_C33 core. From the left, downcore variations versus age of *G. bulloides* $\delta^{18}O$ values and of selected coccolith taxa belonging to the Miscellaneous group. Columns on the left and dashed black lines show the division into marine isotopic stages and substages. Dark grey bands correspond to Heinrich events and MIS 5 cold spells, light grey bands to stadials. YD: Younger Dryas; H1–H6: Heinrich events; S25–S20: MIS 5 cold spells; Hcar base: *H. carteri* base; Hcar top: *H. carteri* top; Shis base: *S. histrica* base; Shis top: *S. histrica* top; Pleur base: *Pleurochrysis* spp. base; Pleur top: *Pleurochrysis* spp. top.

base of the Bolling–Allerød is also detected (Colmenero-Hidalgo et al., 2004; Sierro et al., 2005). The only data available to evaluate the traceability of the Ehux4 base event are from the two cores of the Balearic Sea (Flores et al., 1997). The increase of *E. huxleyi* >4 μm is reported in the middle part of MIS 4 for core K10 (exactly like in Arcose C_33 core) and at the beginning of MIS 4 for core K1.

The *G. muellerae* ecobioevent is defined by the significant decreases in abundance occurred just after the MIS 6/MIS 5 boundary (Gmue top, 125.2 ± 4.0 kyr BP) (Fig. 3). This event is also recognized in the Sicily Channel (Incarbona et al., 2008a, 2010c).

G. oceanica ecobioevents (Goc base1 at 124.2 ± 4.0 kyr BP, Goc top1 at 116.0 ± 4.0 kyr BP and Goc base2 at 11.55 ± 0.1 kyr BP) define intervals (last interglacial sensu lato and Holocene) where this species occurs continuously and with relatively high abundance (Fig. 3). The events that deal with the last interglacial, although minor time discrepancies, can be traced across the Sicily Channel and the close LC07 core (Incarbona et al., 2008a, 2010c), while no data exist from other sites. The significant increase of *G. oceanica* since the Holocene is a widespread event and can be recognized in the Alboran, Balearic and Tyrrhenian Seas and in the Sicily Channel (Flores et al., 1997; Sbaffi et al., 2001; Buccheri et al., 2002; Colmenero-Hidalgo, 2004; Di Stefano and Incarbona, 2004), while it is missing from the Aegean Sea (Triantaphyllou et al., 2009). The marked modification of the original properties of MAW, especially in terms of increased salinity, seems to be the most likely explanation for missing specimens in the eastern Mediterranean (e.g., Knappertsbusch, 1993; Incarbona et al., 2008c).

7.2.2. UPZ and LPZ taxa

The distinct occurrence of *U. sibogae* (Usib base) at 10.4 ± 0.1 kyr BP (Fig. 4) finds an unexpected wide traceability across the Mediterranean Sea, in the Balearic and Tyrrhenian Seas, in the Sicily Channel and in the Aegean Sea (Flores et al., 1997; Sbaffi et al., 2001; Buccheri et al., 2002; Di Stefano and Incarbona, 2004; Triantaphyllou et al., 2009). Less certain is the distribution of this species in the Alboran Sea, because it was grouped into warm water taxa that increase in abundance during the Holocene (Colmenero-Hidalgo et al., 2004).

F. profunda ecobioevents (Fprof base1 at 124.2 ± 4.0 kyr BP, Fprof top1 at 113.0 ± 4.0 kyr BP and Fprof base2 at 11.55 ± 0.1 kyr BP) define intervals where this species occurs continuously and with relatively high abundance within the last interglacial and the Holocene intervals (Fig. 4). They coincide again with the last interglacial sensu lato and the Holocene, even if the Fprof top1 is slightly delayed with respect to Goc top1 (Table 3). Likewise *G. oceanica*, the increase of *F. profunda* during the last interglacial sensu lato can be recognized in the Sicily Channel and the close LC07 core (Incarbona et al., 2008a, 2010c). At the base of the Holocene, *F. profunda* increase in the Balearic and Tyrrhenian Seas and in the Sicily Channel (Flores et al., 1997; Sbaffi et al., 2001; Di Stefano and Incarbona, 2004), even if for the latter two sites there is a significant increase in abundance that also involves the Termination I.

7.2.3. Miscellaneous taxa and holococcoliths

H. carteri, holococcoliths, *Pleurochrysis* spp. and *S. histrica* show wide and repeated abundance fluctuations that span from MIS 4 to MIS 2

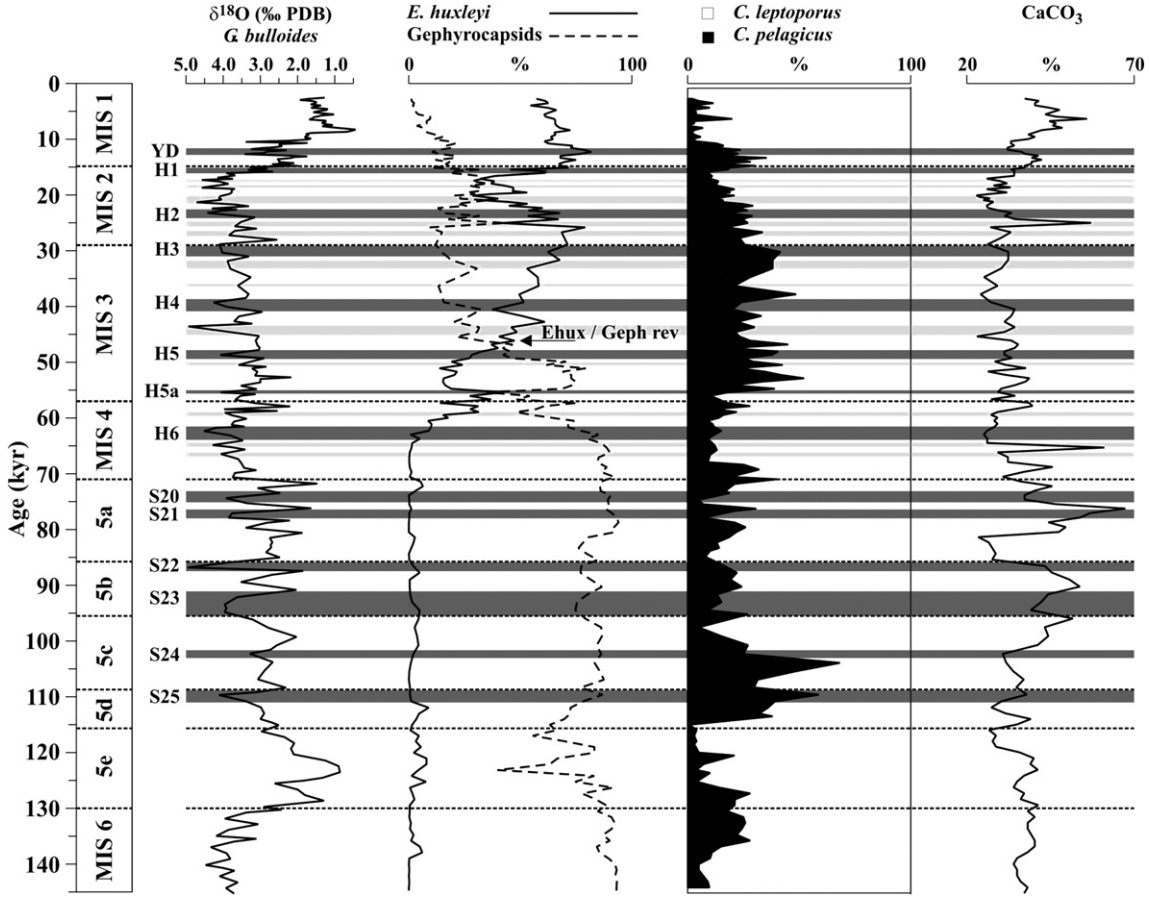

Fig. 6. Geochemical and micropaleontological data in the Arcose_C33 core. From the left, downcore variations versus age of *G. bulloides* $\delta^{18}O$ values, total *E. huxleyi* and gephyrocapsids, the additional counting on 100 specimens of *C. leptoporus* and *C. pelagicus* and the $CaCO_3$ content in the bulk sediment. Columns on the left and dashed black lines show the division into marine isotopic stages and substages. Dark grey bands correspond to Heinrich events and MIS 5 cold spells, light grey bands to stadials. YD: Younger Dryas; H1–H6: Heinrich events; S25–S20: MIS 5 cold spells; Ehux/Geph exch: reversal between *E. huxleyi* and gephyrocapsids specimens.

(Figs 4 and 5). This interval covers the distribution of *E. huxleyi* >4 μm (which is indeed also present during the Younger Dryas, Fig. 3) and the abundance variations of the taxa can be correlated to each other during stadials and Heinrich events with a relevant palaeoecological meaning.

The end of these fluctuations defines four ecobioevents with only minor time discrepancies (Hcar top at 16.0 ± 0.2 kyr BP, Holo top at 15.1 ± 0.2 kyr BP, Pleur top at 16.6 ± 0.3 kyr BP, and Shis top at 16.0 ± 0.2 kyr BP). Significant peaks of *H. carteri* and *S. histrica* have been found in the last glacial interval of the Alboran Sea, and Sicily Channel (Colmenero-Hidalgo et al., 2004; Incarbona et al., 2008a, 2013) and, like in the present study, they stop just before the beginning of the Bolling–Allerød. Objectively, it is difficult to indicate the beginning of significant fluctuations for these taxa: there are significant abundance increases both around He6 and He5 (Figs 4 and 5), and we tentatively place ecobioevents in the lower stratigraphic horizon (Hcar base at 61.7 ± 3.9 kyr BP, Holo base at 62.3 ± 4.0 kyr BP, Pleur base at 64.5 ± 4.2 kyr BP, and Shis base at 61.7 ± 3.9 kyr BP). Looking at data of core LC07 and of ODP Site 963, the correlation of Hcar base and Shis base suffers from the ambiguity due to the small magnitude of initial peaks. In both records, ecobioevents may be traced around H5 (Incarbona et al., 2008a, 2013).

No peaks of such a magnitude have so far been noted in the distribution pattern of holococcoliths and of *Pleurochrysis* spp., including data from the nearby LC07 core (Incarbona et al., 2008a).

7.2.4. Coccolithus pelagicus and Calcidiscus spp.

The abundance reversal between *C. leptoporus* and *C. pelagicus* was reported as a useful biostratigraphic tool by Fenner and Di Stefano (2004) at the MIS 1/2 boundary in both subtropical and subantarctic surface waters. In sediments of the Arcose C_33 core, *C. pelagicus* shows a drastic fall-down at the MIS 1/2 transition and during MIS 1, where *C. leptoporus* is dominant. These results suggest that the relationship between the two species may be useful to approximate the MIS 1 base even in the Mediterranean region.

7.2.5. General comment on the correlation of ecobioevents across the Mediterranean Sea

For the sake of clarity, in Fig. 8 only six events were correlated between the Sardinia Channel record and most of the relevant coccolith studies in the Mediterranean Sea. However, the plots summarize our main results: there is a good correlation of events between the Arcose C_33 core and the Sicily Channel, Tyrrhenian and Balearic Seas, where correlation lines are well within error age estimates. The only event that is apparently diachronous, Hcar base, is definitively due to analytical uncertainty, that is the problematic detection of the beginning of wide abundance fluctuations of miscellaneous taxa. Thus, despite the strong fragmentation of the surface marine ecosystems among different subbasins, due to W–E physico-chemical gradients and meso-scale circulation features (Poem group, 1992), coccolith assemblages behave in a similar way with respect to the most relevant climatic/oceanographic variations, such as the passage from glacial to interglacial conditions. We emphasize that a common ecobiostratigraphic scheme may be drawn for such a large portion of the central-western Mediterranean Sea, where there is apparently little or no influence of local climatic/oceanographic factors.

The correlation with the Alboran Sea seems to be limited to wide abundance fluctuations of *G. oceanica*, *H. carteri* and *S. histrica*. Possibly, the peculiar condition of the westernmost Mediterranean basin is better comparable with high-productive deep formation areas, the Gulf of Lions, Adriatic and Aegean Seas. However, we want to stress the correlation of *H. carteri* and *S. histrica* peaks during stadials and/or Heinrich events among the Sicily Channel, southern Tyrrhenian and

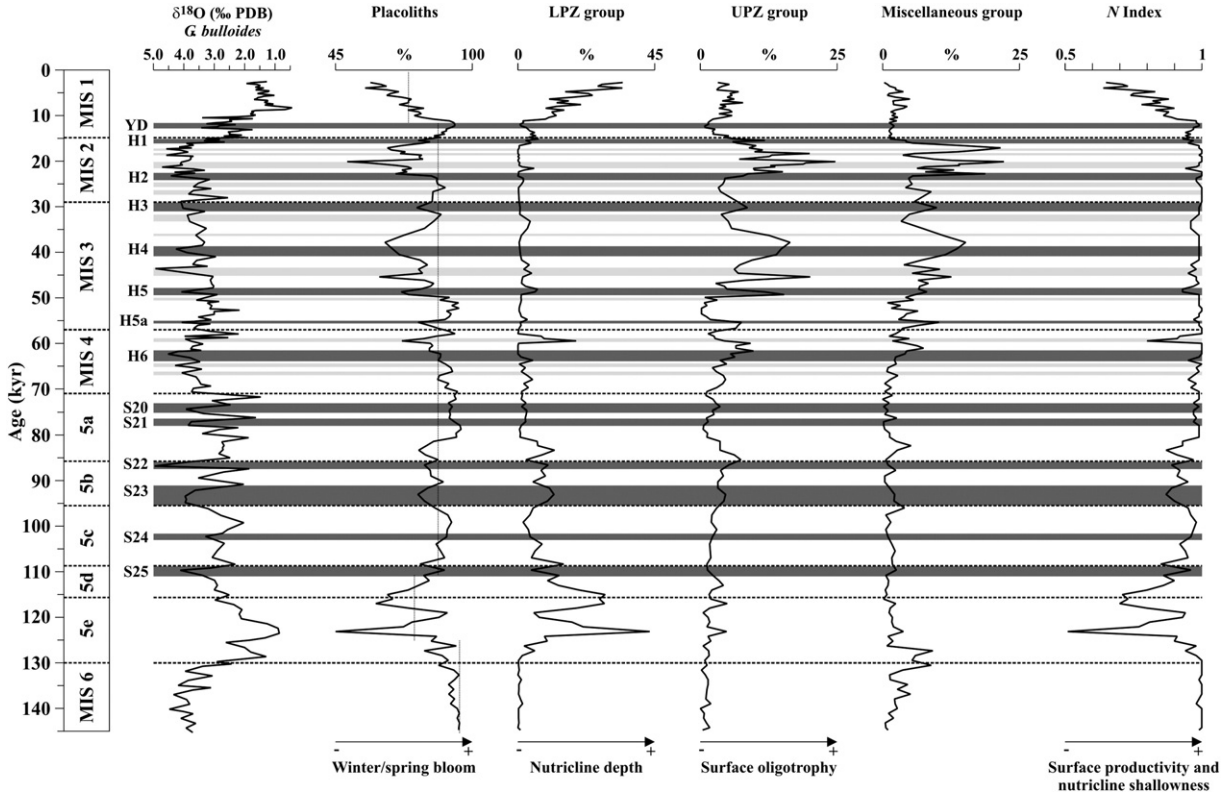

Fig. 7. Geochemical and micropaleontological data in the Arcose_C33 core. From the left, downcore variations versus age of *G. bulloides* $\delta^{18}O$ values, coccolith groups and *N* ratio. Dashed vertical lines within the distribution pattern of placoliths indicate the average values for the intervals of MIS 6, last interglacial, last glacial and Holocene. Columns on the left and dashed black lines show the division into marine isotopic stages and substages. Dark grey bands correspond to Heinrich events and MIS 5 cold spells, light grey bands to stadials. YD: Younger Dryas; H1–H6: Heinrich events; S25–S20: MIS 5 cold spells.

the Alboran Seas. Once again, this fact suggests similar nutrient (and water column) dynamics and the same response of the coccolith community to suborbital climatic variations.

The correlation of ecobioevents with the eastern Mediterranean Sea is rather poor, limited to the occurrence of *U. sibogae* in the Aegean Sea. It is possible that this partly reflects missing high-resolution studies on long sedimentary records, as well as appropriate calcareous investigations focused on issues other than the sapropel theme. However, we strongly suspect that the ultraoligotrophic environment in the eastern basin and the occurrence of a deep chlorophyll maximum coincident with nutricline shallowing into the photic zone, during orbitally-controlled deposition of sapropel layers (Rohling and Gieskes, 1989; Castradori, 1993b; Incarbona et al., 2011), may not have led to the same sequence of ecobioevents observed in western and central Mediterranean sites.

8. Conclusion

The high-resolution quantitative study of coccolith assemblages in the Arcose_C33 core, obtained from the Sentinelle Valley (Sardinia Channel) is herein reported. The record covers the last 145 kyr by an average sampling resolution of about 900 years.

Gephyrocapsids are dominant up to 46.1 ± 1.9 kyr BP, where they are replaced by *E. huxleyi* (Fig. 6). Higher productivity conditions characterise the last glacial period but abundance increases of *H. carteri*, holococcoliths (*S. pulchra* HOL *oblonga*) and *S. histrica* at the expense of the placoliths during Heinrich events and stadials (Figs 4–7) suggest the occurrence of reduced productivity episodes and support previous evidence in the Alboran Sea and Sicily Channel (Cacho et al., 2000, 2002; Pérez-Folgado et al., 2003; Colmenero-Hidalgo et al., 2004; Moreno et al., 2004, 2005; Incarbona et al., 2013). Abundance peaks of *F. profunda* and the turnover within placoliths (i.e. small *Gephyrocapsa*/*G. muellerae*) indicate reduced productivity levels and the development of a deep nutricline during the last interglacial and the Holocene (e.g., Molfino and McIntyre, 1990; Beaufort et al., 1997; Flores et al., 1997, 2000; Henriksson, 2000; Baumann and Freitag, 2004; Incarbona et al., 2008b, 2010c).

A total of 19 ecobioevents were identified in the Sardinia Channel record (Table 3) dealing with significant abundance fluctuations of, among others, *E. huxleyi* >4 μm, *F. profunda*, *G. oceanica*, *H. carteri* and *S. histrica*. The continuity over the last two glacial/interglacial cycles and the high-resolution of the study allow us to evaluate the traceability of the ecobioevents in different Mediterranean sites (Fig. 8). We conclude that a common ecobiostratigraphic scheme may be drawn up for a large portion of the central-western Mediterranean Sea, including Sicily Channel, Tyrrhenian and Balearic Seas. Especially important is also the correlation of peaks of *H. carteri* and *S. histrica* during Heinrich events and stadials that suggests similar nutrient dynamics in response to suborbital climatic variations in the Sicily Channel, southern Tyrrhenian and Alboran Seas. Finally, we point out that the traceability of ecobioevents with the eastern Mediterranean Sea is difficult because of very few studies that cover this stratigraphic interval. The correlation with the only eastern Mediterranean long-record (with a suitable high-resolution and not focused only on sapropel deposition aspects, Triantaphyllou

Table 3
List of the 19 ecobioevents identified in the Arcose_C33 core and a synthetic scheme of their traceability. From the left: Ecobioevent label; age (kyr BP) of each biohorizon; traceability of the event in Mediterranean Sea; bibliographic references used to trace the comparison. 1: Flores et al. (1997); 2: Incarbona et al. (2008a); 3: Incarbona et al. (2013); 4: Colmenero-Hidalgo et al. (2004); 5: Sbaffi et al. (2001); 6: Buccheri et al. (2002); 7: Di Stefano and Incarbona (2004); 8: Colmenero-Hidalgo (2004); 9: Triantaphyllou et al. (2009); 10: Incarbona et al. (2010c).

Ecobioevent	Age (kyr BP)	Traceability	Reference (see caption)
Ehux/Geph rev	46.1 ± 1.9	Balearic, Tyrrhenian, Sicily Channel	1, 2 and 3
Ehux4 top	15.1 ± 0.2	Alboran,	4
Ehux4 base	63.0 ± 4.1	Balearic	1
Gmue top	125.2 ± 4.0	Tyrrhenian, Sicily Channel	2 and 3
Goc base2	11.55 ± 0.1	Balearic, Tyrrhenian, Sicily Channel, Alboran	1, 5, 6, 7 and 8
Goc top1	116.0 ± 4.0	Sicily Channel	2 and 3
Goc base1	124.2 ± 4.0	Sicily Channel	2 and 3
Usib base	10.4 ± 0.1	Balearic, Tyrrhenian, Sicily Channel, Aegean	1, 5, 6, 7 and 9
Fprof base2	11.55 ± 0.1	Balearic, Tyrrhenian, Sicily Channel	1, 5 and 7
Fprof top1	113.0 ± 4.0	Sicily Channel	2 and 10
Fprof base1	124.2 ± 4.0	Sicily Channel	2 and 10
Pleur top	16.6 ± 0.3	No data	
Pleur base	64.5 ± 04.2	No data	
Shis top	16.0 ± 0.2	Alboran, Sicily Channel	2, 3 and 4
Shis base	61.7 ± 3.9	Sicily Channel	2 and 3?
Hcar top	16.0 ± 0.2	Alboran, Sicily Channel	2, 3 and 4
Hcar base	61.7 ± 3.9	Sicily Channel	2 and 3?
Holo top	15.1 ± 0.2	No data	
Holo base	62.3 ± 4.0	No data	

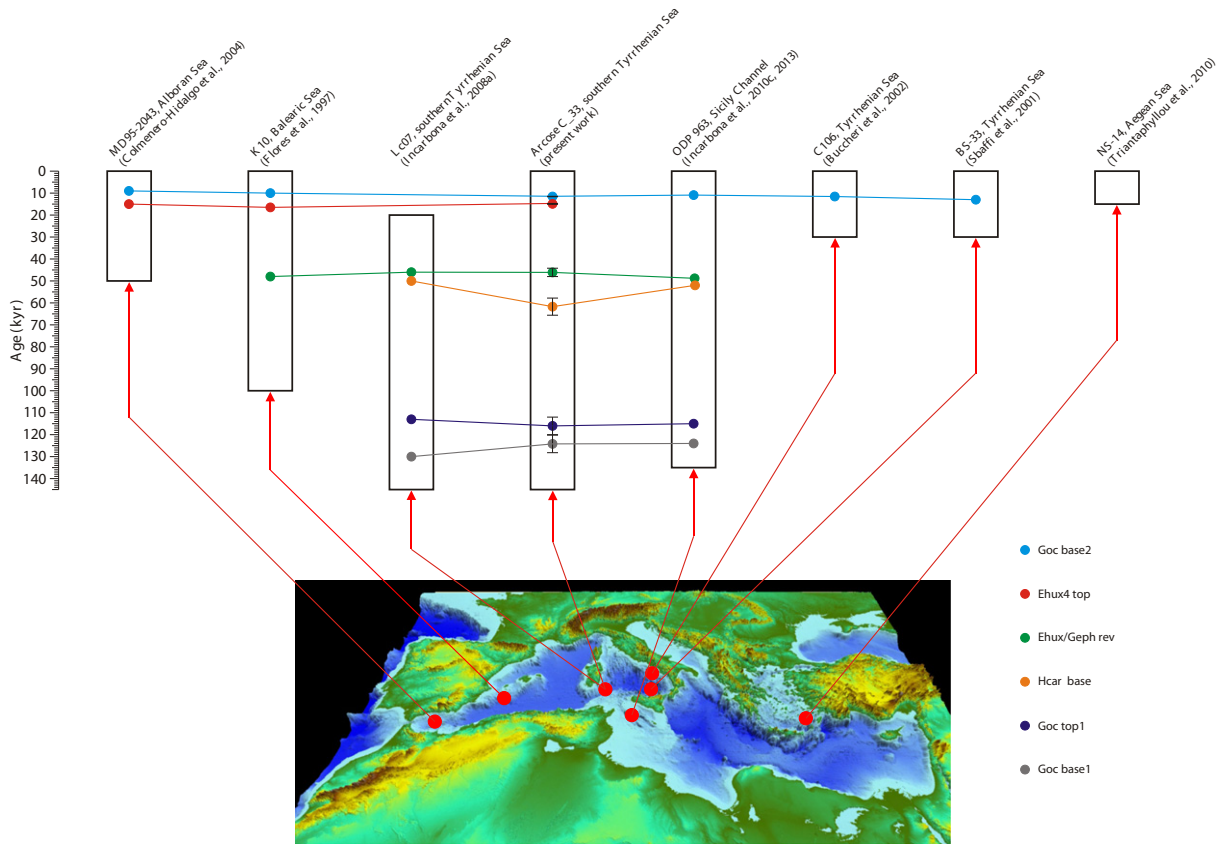

Fig. 8. Traceability of six selected ecobiohorizons across the Mediterranean Sea and core location of coccolith studies used for the comparison. Azure circle: Goc base2 (*G. oceanica* base in the Holocene). Red circle: Ehux4 top (*E. huxleyi* >4 μm top). Green circle: Ehux/Geph exch (reversal between *E. huxleyi* and gephyrocapsids specimens). Orange circle: Hcar base (*H. carteri* base). Blue circle: Goc top1 (*G. oceanica* top in the last interglacial). Grey circle: Goc base1 (*G. oceanica* base in the last interglacial). The error age estimate for Arcose_C33 core is shown. Events for MD95-2043, K10, C106, BS-33 and NS-14 cores are based on the visual inspection of coccolith distribution patterns.

et al., 2009) is rather poor, possibly in spite of the strong west–east thermal and salinity gradient and different nutrient dynamics.

Supplementary data to this article can be found online at http://dx.doi.org/10.1016/j.marmicro.2014.12.002.

Acknowledgments

We are grateful to José-Abel Flores, Richard Jordan and an anonymous reviewer for their valuable comments and suggestions. This work was carried out in the framework of the CNR Arcose Project of the IAMC of Naples (Responsible FB) and also benefited from the financial support of MIUR ex 60% grants awarded to EDS and Ateneo (University of Catania) grants to ADS.

References

Allen, J.R.M., Brandt, U., Brauer, A., Hubberten, H.-W., Huntley, B., Keller, J., Kraml, M., Mackensen, A., Mingram, J., Negendank, J.F.W., Nowaczyk, N.R., Oberhänsli, H., Watts, W.A., Wulf, S., Zolitschka, B., 1999. Rapid environmental changes in southern Europe during the last glacial period. Nature 400, 740–743.

Andruleit, H., Stäger, S., Rogalla, U., Cepek, P., 2003. Living coccolithophores in the northern Arabian Sea: ecological tolerances and environmental control. Mar. Micropaleontol. 49, 157–181.

Astraldi, M., Balopulos, S., Candela, J., Font, J., Gačić, M., Gasparini, G.P., Manca, B., Theocharis, A., Tintorè, J., 1999. The role of straits and channels in understanding the characteristics of Mediterranean circulation. Prog. Oceanogr. 44, 65–108.

Astraldi, M., Gasparini, G.P., Vetrano, A., Vignudelli, S., 2002. Hydrographic characteristics and interannual variability of water masses in the central Mediterranean: a sensitivity test for long-term changes in the Mediterranean Sea. Deep-Sea Res. I 49, 661–680.

Baumann, K.-H., Freitag, T., 2004. Pleistocene fluctuations in the northern Benguela Current system as revealed by coccolith assemblages. Mar. Micropaleontol. 52, 195–215.

Baumann, K.-H., Andruleit, H., Böckel, B., Geisen, M., Kinkel, H., 2005. The significance of extant coccolithophores as indicators of ocean water masses, surface water temperature, and paleoproductivity: a review. Paläontol. Z. 79, 93–112.

Beaufort, L., Lancelot, Y., Camberlin, P., Cayre, O., Vincent, E., Bassinot, F., Labeyrie, L., 1997. Insolation cycles as a major control of equatorial Indian Ocean primary production. Science 278, 1451–1454.

Béranger, K., Mortier, L., Gasparini, G.-P., Gervasio, L., Astraldi, M., Crépon, M., 2004. The dynamics of the Sicily Strait: a comprehensive study from observations and models. Deep-Sea Res. II 51, 411–440.

Bethoux, J.P., Gentili, B., Morin, P., Nicolas, E., Pierre, C., Ruiz-Pino, D., 1999. The Mediterranean Sea: a miniature ocean for climatic and environmental studies and a key for the climatic functioning of the North Atlantic. Prog. Oceanogr. 44, 131–146.

Boeckel, B., Baumann, K.-H., 2004. Distribution of coccoliths in surface sediments of the south-eastern South Atlantic Ocean: ecology, preservation and carbonate contribution. Mar. Micropaleontol. 51, 301–320.

Bonomo, S., Grelaud, M., Incarbona, A., Malinverno, E., Placenti, F., Bonanno, A., Di Stefano, E., Patti, B., Sprovieri, M., Viveri, P., Genovese, S., Rumolo, P., Mazzola, S., Zgozi, S., 2012. Living coccolithophores from the Gulf of Sirte (Southern Mediterranean Sea) during the summer of 2008. Micropaleontology 58, 487–503.

Bown, P.R., 1998. Calcareous nannofossil biostratigraphy. British Micropaleontological Society Publication SeriesKluwer Academic Publishers, Dordrecht, pp. 1–314.

Bown, P.R., Young, J.R., 1998. Techniques. In: Bown, P.R. (Ed.), Calcareous Nannofossil Biostratigraphy. Kluwer Academic Publishers, Dordrecht, Boston, London, pp. 16–32.

Broerse, A.T.C., Ziveri, P., van Hinte, J.E., Honjo, S., 2000. Coccolithophore export production, species composition, and coccolith-$CaCO_3$ fluxes in the NE Atlantic (34°N 21°W and 48°N 21°W). Deep-Sea Res. II 47, 1877–1905.

Buccheri, G., Capretto, G., Di Donato, V., Esposito, P., Ferruzza, G., Pescatore, T., Russo Ermolli, E., Senatore, M.R., Sprovieri, M., Bertoldo, M., Carella, D., Madonia, G., 2002. A high resolution record of the last deglaciation in the southern Tyrrhenian Sea: environmental and climatic evolution. Mar. Geol. 181, 3–34.

Budillon, F., Lirer, F., Iorio, M., Macrì, P., Sagnotti, L., Vallefuoco, M., Ferraro, L., Garziglia, S., Innangi, S., Sahabi, M., Tonielli, R., 2009. Integrated stratigraphic reconstruction for the last 80 kyr in a deep sector of the Sardinia Channel (Western Mediterranean). Deep-Sea Res. II 56, 725–737.

Cacho, I., Grimalt, J.O., Pelejero, C., Canals, M., Sierro, F.J., Flores, J.A., Shackleton, N., 1999. Dansgaard–Oeschger and Heinrich event imprints in Alboran Sea paleotemperatures. Paleoceanography 14, 698–705.

Cacho, I., Grimalt, J.O., Sierro, F.J., Shackleton, N., Canals, M., 2000. Evidence for enhanced Mediterranean thermohaline circulation during rapid climatic coolings. Earth Planet. Sci. Lett. 183, 417–429.
Cacho, I., Grimalt, J.O., Canals, M., 2002. Response of the Western Mediterranean Sea to rapid climatic variability during the last 50,000 years: a molecular biomarker approach. J. Mar. Syst. 33, 253–272.
Castradori, D., 1993a. Calcareous nannofossil biostratigraphy and biochronology in eastern Mediterranean deep-sea cores. Riv. Ital. Paleontol. Stratigr. 99, 107–129.
Castradori, D., 1993b. Calcareous nannofossils and the origin of eastern Mediterranean sapropels. Paleoceanography 8, 459–471.
Colmenero-Hidalgo, E., 2004. Respuesta de las asociaciones de Cocolitoforidos a los cambios climaticos del Cuaternario final - Reconstruccion de la dinamica superficial y climatica del Mediterraneo occidental y del mar de Arabia. (Philosophy Doctor Thesis). Universidad de Salamanca, Spain, pp. 1–255.
Colmenero-Hidalgo, E., Flores, J.-A., Sierro, F.J., Bárcena, M.A., Löwemark, L., Schönfeld, J., Grimalt, J.O., 2004. Ocean surface water response to short-term climate changes revealed by coccolithophores from the Gulf of Cadiz (NE Atlantic) and Alboran Sea (W Mediterranean). Palaeogeogr. Palaeoclimatol. Palaeoecol. 205, 317–336.
Crudeli, D., Young, J.R., Erba, E., Geisen, M., Ziveri, P., de Lange, G.J., Slomp, C.P., 2006. Fossil record of holococcoliths and selected hetero-holococcolith associations from the Mediterranean (Holocene–late Pleistocene): evaluation of carbonate diagenesis and palaeoecological–palaeooceanographic implications. Palaeogeogr. Palaeoclimatol. Palaeoecol. 237, 191–224.
D'Ortenzio, F., Ribera d'Alcalà, M., 2009. On the trophic regimes of the Mediterranean Sea: a satellite analysis. Biogeosciences 6, 139–148.
De Bernardi, B., Ziveri, P., Erba, E., Thunell, R.C., 2005. Coccolithophore export production during the 1997–1998 El Niño event in Santa Barbara Basin (California). Mar. Micropaleontol. 55, 107–125.
de Jesús Salas Pérez, J., 2003. Evolution of the open-sea eddy ALGERS'98 in the Algerian Basin with Lagrangian trajectories and remote sensing observations. J. Mar. Syst. 43, 105–131.
de Kaenel, E., Siesser, W.G., Murat, A., 1999. Pleistocene calcareous nannofossil Biostratigraphy and the Western Mediterranean sapropels, Sites 974, 977 and 979. In: Zahn, R., Comas, M.C., Klaus, A. (Eds.), Proceedings of the Ocean Drilling Program. Scientific Results 161, pp. 159–183.
Di Stefano, E., 1998. Calcareous nannofossil quantitative biostratigraphy of Holes 963E and 963B (Eastern Mediterranean). In: Emeis, K.-C., Robertson, A.H.F., Richter, C., Camerlenghi, A. (Eds.), Proceedings of the Ocean Drilling Program. Scientific Results 160, pp. 99–112.
Di Stefano, E., Incarbona, A., 2004. High resolution palaeoenvironmental reconstruction of the ODP-963D Hole (Sicily Channel) during the last deglaciation, based on calcareous nannofossils. Mar. Micropaleontol. 52, 241–254.
Di Stefano, A., Verducci, M., Lirer, F., Ferraro, L., Iaccarino, S.M., Hüsing, S.K., Hilgen, F.J., 2010. Palaeoenvironmental conditions preceding the Messinian Salinity Crisis in the Central Mediterranean: integrated data from the Upper Miocene Trave section (Italy). Palaeogeogr. Palaeoclimatol. Palaeoecol. http://dx.doi.org/10.1016/j.palaeo.2010.07.012.
Fenner, J., Di Stefano, A., 2004. Late Quaternary oceanic fronts along Chatham Rise indicated by phytoplankton assemblages, and refined calcareous nannofossil stratigraphy for the mid-latitude SW Pacific. Mar. Geol. 205, 59–86.
Flores, J.-A., Sierro, F.J., Francés, G., Vázquez, A., 1997. The last 100,000 years in the western Mediterranean: sea surface water and frontal dynamics as revealed by coccolithophores. Mar. Micropaleontol. 29, 351–366.
Flores, J.-A., Bárcena, M.A., Sierro, F.J., 2000. Ocean-surface and wind dynamics in the Atlantic Ocean off Northwest Africa during the last 140,000 years. Palaeogeogr. Palaeoclimatol. Palaeoecol. 161, 459–478.
Flores, J.-A., Colmenero-Hidalgo, E., Mejía-Molina, A., Baumann, K.-H., Henderiks, J., Larsson, K., Prabhu, C.N., Sierro, F.J., Rodrigues, T., 2010. Distribution of large *Emiliania huxleyi* in the Central and Northeast Atlantic as a tracer of surface ocean dynamics during the last 25,000 years. Mar. Micropaleontol. 76, 53–66.
Frigola, J., Moreno, A., Cacho, I., Canals, M., Sierro, F.J., Flores, J.A., Grimalt, J.O., 2008. Evidence of abrupt changes in Western Mediterranean Deep Water circulation during the last 50 kyr: a high-resolution marine record from the Balearic Sea. Quat. Int. 181, 88–104.
Giraudeau, J., 1992. Distribution of recent nannofossils beneath the Benguela system: southwest African continental margin. Mar. Geol. 108, 219–237.
Grelaud, M., Marino, G., Ziveri, P., Rohling, E.J., 2012. Abrupt shoaling of the nutricline in response to massive freshwater flooding at the onset of the last interglacial sapropel event. Paleoceanography 27. http://dx.doi.org/10.1029/2012PA002288.
Henriksson, A.S., 2000. Coccolithophore response to oceanographic changes in the equatorial Atlantic during the last 200,000 years. Palaeogeogr. Palaeoclimatol. Palaeoecol. 156, 161–173.
Hilgen, F.J., 1987. Sedimentary rhythms and high-resolution chronostratigraphic correlation in the Mediterranean Pliocene. Newslett. Stratigr. 17, 109–127.
Hilgen, F.J., 1991. Extension of the astronomically calibrated (polarity) time scale to the Miocene/Pliocene boundary. Earth Planet. Sci. Lett. 104, 211–225.
Incarbona, A., Bonomo, S., Di Stefano, E., Zgozi, S., Essarbout, N., Talha, M., Tranchida, G., Bonanno, A., Patti, B., Placenti, F., Buscaino, G., Cuttitta, A., Basilone, G., Bahri, T., Massa, F., Censi, P., Mazzola, S., 2008a. Calcareous nannofossil surface sediment assemblages from the Sicily Channel (central Mediterranean Sea): palaeoceanographic implications. Mar. Micropaleontol. 67, 297–309.
Incarbona, A., Di Stefano, E., Sprovieri, R., Bonomo, S., Censi, P., Dinarès-Turell, J., Spoto, S., 2008b. Variability in the vertical structure of the water column and Paleoproductivity reconstruction in the Central-Western Mediterranean during the Late Pleistocene. Mar. Micropaleontol. 69, 26–41.
Incarbona, A., Di Stefano, E., Patti, B., Pelosi, N., Bonomo, S., Mazzola, S., Sprovieri, R., Tranchida, G., Zgozi, S., Bonanno, A., 2008c. Holocene millennial-scale productivity variations in the Sicily Channel (Mediterranean Sea). Paleoceanography 23 (PA3204), 1–18. http://dx.doi.org/10.1029/2007PA001581.
Incarbona, A., Di Stefano, E., Bonomo, S., 2009. Calcareous nannofossil biostratigraphy of the Central Mediterranean Basin during the last 430 000 years. Stratigraphy 6, 33–44.
Incarbona, A., Bonomo, S., Di Stefano, E., Sprovieri, R., Pelosi, N., Sprovieri, M., 2010a. Millennial-scale palaeoenvironmental changes in the central Mediterranean during the Last Interglacial: comparison with European and Mediterranean records. Geobios 43, 111–122.
Incarbona, A., Ziveri, P., Di Stefano, E., Lirer, F., Mortyn, G., Patti, B., Pelosi, N., Sprovieri, M., Tranchida, G., Vallefuoco, M., Albertazzi, S., Bellucci, L.G., Bonanno, A., Bonomo, S., Censi, P., Ferraro, L., Giuliani, S., Mazzola, S., Sprovieri, R., 2010b. The Impact of the Little Ice Age on coccolithophores in the Central Mediterranean Sea. Clim. Past 6, 795–805.
Incarbona, A., Martrat, B., Di Stefano, E., Grimalt, J.O., Pelosi, N., Patti, B., Tranchida, G., 2010c. Primary productivity variability on the Atlantic Iberian Margin over the last 70,000 years: evidence from coccolithophores and fossil organic compounds. Paleoceanography 25 (PA2218), 1–15. http://dx.doi.org/10.1029/2008PA001709.
Incarbona, A., Ziveri, P., Sabatino, N., Salvagio Manta, D., Sprovieri, M., 2011. Conflicting coccolithophore and geochemical evidence for productivity levels in the Eastern Mediterranean sapropel S1. Mar. Micropaleontol. 81, 131–143.
Incarbona, A., Sprovieri, M., Di Stefano, A., Di Stefano, E., Salvagio Manta, D., Pelosi, N., Ribera d'Alcalà, M., Sprovieri, R., Ziveri, P., 2013. Productivity modes in the Mediterranean Sea during Dansgaard–Oeschger (20,000–70,000 yr ago) oscillations. Palaeogeogr. Palaeoclimatol. Palaeoecol. 392, 128–137.
Iorio, M., Liddicoat, J., Budillon, F., Incoronato, A., Coe, R.S., Insinga, D.D., Cassata, W.S., Lubritto, C., Angelino, A., Tamburrino, S., 2014. Combined palaeomagnetic secular variation and petrophysical records to time-constrain geological and hazardous events: an example from the eastern Tyrrhenian Sea over the last 120 ka. Glob. Planet. Chang. 112. http://dx.doi.org/10.1016/j.gloplacha.2013.11.005.
Jordan, R.W., Zhao, M., Eglinton, G., Weaver, P.P.E., 1996. Coccolith and alkenone stratigraphy and palaeoceanography at an upwelling site off NW Africa (ODP 658C) during the last 130,000 years. In: Moguilevsky, A., Whatley, R. (Eds.), Microfossils and Oceanic Environments. University of Wales Press, Aberystwyth, pp. 111–130.
Kleijne, A., 1991. Holococcolithophorids from the Indian Ocean, Red Sea, Mediterranean Sea and North Atlantic Ocean. Mar. Micropaleontol. 17, 1–76.
Klein, P., Coste, P., 1984. Effects of wind stress variability on nutrient transport into the mixed layer. Deep-Sea Res. 31, 21–37.
Knappertsbusch, M., 1993. Geographic distribution of living and Holocene coccolithophores in the Mediterranean Sea. Mar. Micropaleontol. 21, 219–247.
Krom, M.D., Kress, N., Brenner, S., Gordon, L.I., 1991. Phosphorus limitation of primary productivity in the Eastern Mediterranean Sea. Limnol. Oceanogr. 36, 424–432.
Krom, M.D., Brenner, N.K., Neori, A., Gordon, L.I., 1992. Nutrient dynamics and new production in a warm-core eddy from the Eastern Mediterranean Sea. Deep-Sea Res. 39, 467–480.
Krom, M.D., Emeis, K.-C., Van Cappellen, P., 2010. Why is the Eastern Mediterranean phosphorus limited? Prog. Oceanogr. 85, 236–244.
Lirer, F., Sprovieri, M., Ferraro, L., Vallefuoco, M., Capotondi, L., Cascella, A., Petrosino, P., Insinga, D.D., Pelosi, N., Tamburrino, S., Lubritto, C., 2013. Integrated stratigraphy for the Late Quaternary in the eastern Tyrrhenian Sea. Quat. Int. 292, 71–85.
Lisiecki, L.E., Raymo, M.E., 2005. Pliocene–Pleistocene stack of 57 globally distributed benthic δ18O records. Paleoceanography 20. http://dx.doi.org/10.1029/2004PA001071.
López-Otálvaro, G.E., Flores, J.A., Sierro, F.J., Cacho, I., 2008. Variations in coccolithophorid production in the Eastern Equatorial Pacific at ODP Site 1240 over the last seven glacial–interglacial cycles. Mar. Micropaleontol. 69, 52–69.
Malanotte-Rizzoli, P., Hecht, A., 1988. Large scale properties of the Eastern Mediterranean: a review. Oceanol. Acta 11, 323–335.
Malanotte-Rizzoli, P., Artale, V., Borzelli-Eusebi, G.L., Brenner, S., Civitarese, G., Crise, A., Font, J., Gacic, M., Kress, N., Marullo, S., Ozsoy, E., Ribera d'Alcalà, M., Roether, W., Schroeder, K., Sofianos, S., Tanhua, T., Theocharis, A., Alvarez, M., Ashkenazy, Y., Bergamasco, A., Cardin, V., Carniel, S., D'Ortenzio, F., Garcia-Ladona, E., Garcia-Lafuente, J.M., Gogou, A., Gregoire, M., Hainbucher, D., Kontoyannis, H., Kovacevic, V., Krasakapoulou, E., Krokos, G., Incarbona, A., Mazzocchi, M.G., Orlic, M., Pascual, A., Poulain, P.M., Rubino, A., Siokou-Frangou, J., Souvermezoglou, E., Sprovieri, M., Tintorè, J., Triantafyllou, G., 2014. Physical forcing and physical/biochemical variability of the Mediterranean Sea: a review of unresolved issues and directions for future research. Ocean Sci. 10, 281–322.
Malinverno, E., Triantaphyllou, M.V., Stavrakakis, S., Ziveri, P., Lykousis, V., 2009. Seasonal and spatial variability of coccolithophore export production at the South-Western margin of Crete (Eastern Mediterranean). Mar. Micropaleontol. 71, 131–147.
Martrat, B., Grimalt, J.O., Lopez-Martinez, C., Cacho, I., Sierro, F.J., Flores, J.A., Zahn, R., Canals, M., Curtis, J.H., Hodell, D.A., 2004. Abrupt temperature changes in the Western Mediterranean over the past 250,000 years. Science 306, 1762–1765.
Millot, C., 1999. Circulation in the western Mediterranean Sea. J. Mar. Syst. 20, 423–442.
Molfino, B., McIntyre, A., 1990. Precessional forcing of nutricline dynamics in the Equatorial Atlantic. Science 249, 766–769.
Moreno, A., Cacho, I., Canals, M., Grimalt, J.O., 2004. Millennial-scale variability in the productivity signal from the Alboran Sea record. Palaeogeogr. Palaeoclimatol. Palaeoecol. 211, 205–219.
Moreno, A., Cacho, I., Canals, M., Grimalt, J.O., Sánchez-Goñi, M.-F., Shackleton, N., Sierro, F.J., 2005. Links between marine and atmospheric processes oscillating on a millennial time-scale. A multi-proxy study of the last 50,000 yr from the Alboran Sea (Western Mediterranean Sea). Quat. Sci. Rev. 24, 1623–1636.
Negri, A., Capotondi, L., Keller, J., 1999. Calcareous nannofossils, planktonic foraminifera and oxygen isotopes in the late Quaternary sapropels of the Ionian Sea. Mar. Geol. 157, 89–103.

North Greenland Ice Core Project members, 2004. High-resolution record of Northern Hemisphere climate extending into the last interglacial period. Nature 431, 148–151.
Okada, H., McIntyre, A., 1979. Seasonal distribution of modern coccolithophores in the western North Atlantic Ocean. Mar. Biol. 54, 319–328.
Onken, R., Sellschopp, J., 2001. Water masses circulation between the eastern Algerian Basin and the Strait of Sicily in October 1996. Oceanol. Acta 24, 151–166.
Oppo, D.W., 1997. Millennial climate oscillations. Science 278, 1244–1246.
Ovchinnikov, I.M., 1984. The formation of intermediate water in the Mediterranean. Oceanology 24, 168–173.
Parente, A., Cachão, M., Baumann, K.-H., de Abreu, L., Ferreira, J., 2004. Morphometry of *Coccolithus pelagicus* s.l. (Coccolithophore, Haptophyta) from offshore Portugal, during the last 200 kyr. Micropaleontology 50, 107–120.
Pérez-Folgado, M., Sierro, F.J., Flores, J.-A., Cacho, I., Grimalt, J.O., Zahn, R., 2003. Western Mediterranean planktonic foraminifera events and climatic variability during the last 70 kyr. Mar. Micropaleontol. 48, 49–70.
Pinardi, N., Masetti, E., 2000. Variability of the large scale general circulation of the Mediterranean Sea from observations and modelling: a review. Palaeogeogr. Palaeoclimatol. Palaeoecol. 158, 153–174.
POEM group, 1992. General circulation of the Eastern Mediterranean. Earth Sci. Rev. 32, 285–309.
Principato, M.S., Crudeli, D., Ziveri, P., Slomp, C.P., Corselli, C., Erba, E., de Lange, G.J., 2006. Phyto- and zooplankton paleofluxes during the deposition of sapropel S1 (eastern Mediterranean): biogenic carbonate preservation and paleoecological implications. Palaeogeogr. Palaeoclimatol. Palaeoecol. 235, 8–27.
Pujos, A., 1988. Spatio-temporal distribution of some Quaternary coccoliths. Oceanol. Acta 11, 65–77.
Quinn, P.S., Sáez, A.G., Baumann, K.-H., Steel, B.A., Sprengel, C., Medlin, L.K., 2004. Coccolithophorid biodiversity: evidence from the cosmopolitan species *Calcidiscus leptoporus*. In: Thierstein, H.R., Young, J.R. (Eds.), Coccolithophores. From Molecular Processes to Global Impact. Springer-Verlag, Heidelberg, pp. 299–326.
Raffi, I., Backman, J., Rio, D., Shackleton, N.J., 1993. Plio-Pleistocene nannofossil biostratigraphy and calibration to oxygen isotopes stratigraphies from Deep Sea Drilling Project Site 607 and Ocean Drilling Program Site 677. Paleoceanography 8, 387–408.
Rey, J., Galeotti, S., 2008. Biostratigraphy. In: Ray, J., Galeotti, S. (Eds.), Stratigraphy — Terminology and Practice. Technip editor, Paris, pp. 65–90.
Rio, D., 1982. The fossil distribution of coccolithophore genus *Gephyrocapsa* Kamtner and related Plio-Pleistocene chronostratigraphic problems. Deep-Sea Drilling Project Initial Reports 68, pp. 325–343.
Rio, D., Raffi, I., Villa, G., 1990. Pliocene–Pleistocene calcareous nannofossil distribution patterns in the western Mediterranean. In: Kastens, K.A. (Ed.), Proceedings of the Ocean Drilling Program. Scientific Results 107, pp. 513–533.
Robinson, A.R., Sellschopp, J., Warn-Varnas, A., Leslie, W.G., Lozano, C.J., Haley Jr., P.J., Anderson, L.A., Lermusiaux, P.F.J., 1999. The Atlantic Ionian Stream. J. Mar. Syst. 20, 129–156.
Rogalla, U., Andruleit, H., 2005. Precessional forcing of coccolithophore assemblages in the northern Arabian Sea: implications for monsoonal dynamics during the last 200,000 years. Mar. Geol. 217, 31–48.
Rohling, E.J., Gieskes, W.W.C., 1989. Late Quaternary changes in Mediterranean Intermediate Water density and formation rate. Paleoceanography 4, 531–545.
Roth, P.H., Coulbourne, W.T., 1982. Floral and solution patterns of coccoliths in surface sediments of the North Pacific. Mar. Micropaleontol. 7, 1–52.
Sammari, C., Millot, C., Taupier-Letage, I., Stefani, A., Brahim, M., 1999. Hydrological characteristics in the Tunisia–Sardinia–Sicily area during spring 1995. Deep-Sea Res. I 46, 1671–1703.
Samtleben, C., 1980. Die evolution der coccolithophoriden - gattung *Gephyrocapsa* nach befunden im Atlantik. Paläontol. Zh. 54, 91–127.
Sanchez Goñi, M.F., Eynaud, F., Turon, J.L., Shackleton, N.J., 1999. High resolution palynological record off the Iberian margin: direct land–sea correlation for the Last Interglacial complex. Earth Planet. Sci. Lett. 171, 123–137.
Sbaffi, L., Wezel, F.C., Kallel, N., Paterne, M., Cacho, I., Ziveri, P., Shackleton, N., 2001. Response of the pelagic environment to palaeoclimatic changes in the central Mediterranean Sea during the Late Quaternary. Mar. Geol. 178, 39–62.
Schulz, M., Statteger, K., 1997. SPECTRUM: a PC-program for spectral analysis of unevenly spaced time series, INQUA Sub-Comm. Data-Handl. Methods Newsl 16 (Available at http://www.kv.geo.uu.se/inqua/news16/n16-ms1.htm).
Shackleton, N.J., Sanchez Goñi, M.F., Pailler, D., Lancelot, Y., 2003. Marine Isotope 5e and the Eemian Interglacial. Glob. Planet. Chang. 36, 151–155.
Sierro, F.J., Hodell, D.A., Curtis, J.H., Flores, J.-A., Reguera, I., Colmenero-Hidalgo, E., Bárcena, M.A., Grimalt, J.O., Cacho, I., Frigola, J., Canals, M., 2005. Impact of iceberg melting on Mediterranean thermohaline circulation during Heinrich Events. Paleoceanography 20. http://dx.doi.org/10.1029/2004PA001051.
Spötl, C., Vennemann, T.W., 2003. Continuous-flow isotope ratio mass spectrometric analysis of carbonate minerals. Rapid Commun. Mass Spectrom. 17, 1004–1006.
Sprovieri, R., Di Stefano, E., Incarbona, A., Gargano, M.E., 2003. A high-resolution record of the last deglaciation in the Sicily Channel based on foraminifera and calcareous nannofossil quantitative distribution. Palaeogeogr. Palaeoclimatol. Palaeoecol. 202, 119–142.
Sprovieri, R., Di Stefano, E., Incarbona, A., Oppo, D.W., 2006. Suborbital climate variability during Marine Isotopic Stage 5 in the central Mediterranean Basin: evidence from calcareous plankton. Quat. Sci. Rev. 25, 2332–2342.
Sprovieri, M., Di Stefano, E., Incarbona, A., Salvagio Manta, D., Pelosi, N., Ribera d'Alcalà, M., Sprovieri, R., 2012. Centennial- to millennial-scale oscillations in the Central-Eastern Mediterranean Sea between 20,000 and 70,000 years ago: evidence from a high-resolution geochemical and micropaleontological record. Quat. Sci. Rev. 46, 126–135.
Takahashi, K., Okada, H., 2000. Environmental control on the biogeography of modern coccolithophores in the southeastern Indian Ocean offshore of Western Australia. Mar. Micropaleontol. 39, 73–86.
Tangen, K., Brand, L.E., Blackwelder, P.L., Guillard, R.R.L., 1982. *Thoracosphaera heimii* (Lohmann) Kamptner is a dinophyte: observations on its morphology and life cycle. Mar. Micropaleontol. 7, 193–212.
Thierstein, H.R., Geitzenauer, K.R., Molfino, B., Shackleton, N.J., 1977. Global synchroneity of late Quaternary coccolith datum levels: validation by oxygen isotopes. Geology 5, 400–404.
Toucanne, S., Jouet, G., Ducassou, E., Bassetti, M.-A., Dennielou, B., Angue Minto'o, C.M., Lahmi, M., Touyet, N., Charlier, K., Lericolais, G., Mulder, T., 2012. A 130,000-year record of Levantine Intermediate Water flow variability in the Corsica Trough, western Mediterranean Sea. Quat. Sci. Rev. 33, 55–73.
Triantaphyllou, M.V., Antonarakou, A., Kouli, K., Dimiza, M., Kontakios, G., Papanikolaou, M.D., Ziveri, P., Mortyn, P.G., Lianou, V., Lykousis, V., Dermitzakis, M.D., 2009. Late Glacial–Holocene ecostratigraphy of the south-eastern Aegean Sea, based on plankton and pollen assemblages. Geo-Mar. Lett. 29, 249–267.
Villanueva, J., Flores, J.A., Grimalt, J.O., 2002. A detailed comparison of the UK'37 and coccolith records over the past 290 kyears: implications to the alkenone paleotemperature method. Org. Geochem. 33, 897–905.
Winter, A., Jordan, R.W., Roth, P.H., 1994. Biogeography of living coccolithophores in ocean waters. In: Winter, A., Sissier, W.G. (Eds.), Coccolithophores. Cambridge University Press, Cambridge, pp. 199–218.
Young, J.R., 1994. Functions of coccoliths. In: Winter, A., Siesser, W.G. (Eds.), Coccolithophores. Cambridge University Press, Cambridge, pp. 63–82.
Young, J.R., Geisen, M., Cros, L., Kleijne, A., Sprengel, C., Probert, I., Østergaard, J.B., 2003. A guide to extant coccolithophore taxonomy. J. Nannoplankton Res. Spec. Issue 1, 1–121.